Geometric Morphometric Analysis and Taxonomic Revision of the Gzhelian (Late Pennsylvanian) Conodont Idiognathodus simulator from North America

Authors: Hogancamp, Nicholas J., Barrick, James E., and Strauss, Richard E.

Geometric morphometric analysis and taxonomic revision of the Gzhelian (Late Pennsylvanian) conodont *Idiognathodus simulator* from North America

NICHOLAS J. HOGANCAMP, JAMES E. BARRICK, and RICHARD E. STRAUSS

A new morphometric approach was developed to study morphological variation within P_1 elements commonly referred to as *Idiognathodus simulator*, which was selected to be the biostratigraphic marker for the base of the global Gzhelian Stage (Carboniferous). This new approach combines landmark-based geometric morphometrics with eigen analyses to analyze shape variation within P_1 elements of the *I. simulator* group, and could be used to analyze shape variation in other morphologically similar conodont groups. Specimens analyzed were obtained from three sections of the early Gzhelian Heebner Shale of the Oread cyclothem in the North American Midcontinent region, the cyclothem from which *I. simulator* was originally named. This analysis shows that the *I. simulator* group comprises a set of at least five species with asymmetrical P_1 element pairs, relatively short adcarinal ridges, and a variably developed eccentric groove. Species discrimination is based on the presence of caudal and rostral lobes, character of the adcarinal ridges, and platform shape. The species *I. simulator* is restricted to P_1 elements with a caudal adcarinal ridge that is isolated from the caudal platform margin. *Idiognathodus lateralis* sp. nov. is erected to include P_1 elements with a caudal adcarinal ridge that is not isolated from the caudal platform margin.

Key words: Conodonta, *Idiognathodus*, morphometrics, Pennsylvanian, Gzhelian, North America, Midcontinent.

Nicholas J. Hogancamp [hogancampnj@gmail.com], Department of Geosciences, Texas Tech University, Lubbock, Texas 79409, USA; current address: Hess Corporation, 1501 McKinney Street, Houston, Texas 77010, USA.
James E. Barrick [jim.barrick@ttu.edu], Department of Geosciences, Texas Tech University, Lubbock, Texas 79409, USA.
Richard E. Strauss [Rich.Strauss@ttu.edu], Department of Biological Sciences, Texas Tech University, Lubbock, Texas 79409, USA.

Introduction

Recently the conodont species *Idiognathodus simulator* (Ellison, 1941) was chosen to be the marker species for the base of the global Gzhelian stage (Heckel et al. 2008). Because of this decision, the *I. simulator* group and closely related species will be used for the correlation of the Kasimovian-Gzhelian boundary around the world. Since the original description of *I. simulator* by Ellison (1941) from Midcontinent North America, additional species bearing an eccentric groove like *I. simulator* have been described and named from different regions (Donets Basin, Kozitskaya et al. 1978; south China, Wang and Qi 2003; southern Urals, Chernykh 2005, 2012). This study presents a new geometric morphometric analysis that provides a clearer understand-ing of morphological variation among P_1 elements of the *I. simulator* group recovered from the Heebner Shale of the Oread cyclothem, the oldest Gzhelian cyclothem in the North American Midcontinent region. This new information permits a taxonomic revision that incorporates species concepts from all geographic regions and provides a more precise description of the diagnostic characteristics of *I. simulator* that will facilitate more accurate and precise correlation of the base of the Gzhelian Stage.

Institutional abbreviations.—SUI, University of Iowa Paleontology Repository, Iowa City, USA.

Other abbreviations.—CVA, canonical variate analysis; PCA, principal component analysis; SSCP, square roots and cross products; TT, morphometric identification number.

Historical background

Ellison (1941) erected *Streptognathodus simulator* and *Streptognathodus eccentricus* based on the possession of an eccentric groove that runs down the oral surface of the platform, a feature that distinguished them from other species of *Streptognathodus,* in which the groove, or trough, is medial in position. The feature used to differentiate these two species from each other was that *S. simulator* possessed nodes on only the caudal side of the P_1 element, and *S. eccentricus* possessed nodes on both sides of the P_1 element. *Streptognathodus simulator* was described from the early Virgilian Heebner Shale of the Oread Limestone of Midcontinent North America, and *S. eccentricus* was described from the early Missourian Hushpuckney Shale Member of the Swope Limestone (Ellison 1941). Ellison (1941) reported that *S. eccentricus* ranged through most of the Missourian into the Virgilian, and that *S. simulator* ranged from the late Missourian into the Early Permian. For approximately the next five decades, Ellison's (1941) species concepts were followed by most workers. Kozitskaya et al. (1978) added a third species to the *I. simulator* group from Upper Pennsylvanian strata in the Donets Basin, Ukraine, describing the species *S. luganicus*, which possesses the eccentric groove, but lacks nodes completely and has platform margins that extend ventrally parallel to the carina.

Barrick and Boardman (1989) proposed that *Streptognathodus eccentricus* did not belong to the genus *Streptognathodus*, but was actually a distinct early Missourian form of *Idiognathodus* that was older than the first appearance of the genus *Streptognathodus* in the middle Missourian. This argument was based on their restriction of *Streptognathodus* to a clade of species that appeared in the middle Missourian, and the exclusion of other similar, but unrelated grooved species from the genus (Rosscoe and Barrick 2009). This was in contrast to the general practice, following Ellison (1941), of including all idiognathodids with any groove on the oral surface in *Streptognathodus* and those without a groove to *Idiognathodus*. Barrick and Boardman (1989) removed the species *S. simulator* from *Streptognathodus*, and assigned it to *Idiognathodus* on the basis that it is a member of a unique late Missourian and early Virgilian lineage of *Idiognathodus* unrelated to *Streptognathodus*, characterized by an eccentric groove on the oral platform surface. Barrick and Boardman (1989) reported that *I. simulator* ranged from the Missourian Eudora Shale to the Virgilian Heebner Shale and noted that specimens of *I. simulator* from the Eudora Shale could be differentiated from specimens from the Heebner Shale. Subsequent work in North America (e.g., Boardman and Heckel 1989; Heckel 1989, 2002; Ritter 1995) generally followed these reassignments. In their summary of Midcontinent conodont biostratigraphy, Barrick et al. (2004) modified the nomenclature to distinguish between the older and younger examples of *I. simulator*, using *I.* aff. *simulator* for the Eudora Shale specimens and *I. simulator* (sensu stricto) for the Heebner Shale specimens.

Around this time workers from other regions also began to describe faunas containing *Idiognathodus simulator*-like specimens. Wang and Qi (2003) proposed the species *Streptognathodus luosuensis* to include specimens that have a deflected carina. This species was described from the Nashui (Naqing) section in Guizhou Province, South China. Wang and Qi (2003) recorded *S. luosuensis* as being present only in the *S. simulator* Conodont Zone.

Chernykh (2005) added three new species to the *Idiognathodus simulator* group based on late Kasimovian and early Gzhelian specimens from the southern Urals. Specimens with a short, outward flaring rostral adcarinal ridge were designated as *S. auritus*, and specimens with a straight platform shape as *S. praenuntius*. For *S. praenuntius,* the groove was described as medial and less developed and the platform edges were described as having high ridges and ventral extensions shorter than those typical of *I. eudoraensis*, but longer than *I. simulator*. *Streptognathodus sinistrum* was distinguished from *I. simulator* by a slender platform, a high caudal ridge, and a deep trough separating the caudal ridge from the rest of the platform. Chernykh (2005) illustrated only dextral elements of *S. auritus* and *S. praenuntius* and sinistral elements of *S. sinistrum*. Additional discussion about these species from the Urals can be found in Chernykh et al. (2006) and Davydov et al. (2008).

Barrick et al. (2008) eventually named the older North American species, *Idiognathodus* aff. *simulator*, as *I. eudoraensis* and referred to *I. simulator* (sensu stricto) as simply *I. simulator.* Barrick et al. (2008) described *I. simulator* as an asymmetrical pair of P_1 elements. The sinistral element platforms are curved, have a well-developed eccentric groove, and short adcarinal ridges that occasionally fuse with nodes and lack ventral extensions. The dextral elements are relatively straight, arrowhead-shaped, have a less developed eccentric groove, and a flatter oral surface than the sinistral elements, and both adcarinal ridges lack ventral extensions. Barrick et al. (2008) based the new species *I. eudoraensis* on asymmetrical pairs of P_1 elements that occur in the Eudora Shale of Midcontinent North America, which they distinguished from the *I. simulator* that occurs in the younger Heebner Shale. The sinistral elements of *I. eudoraensis* are relatively straight, have a slightly developed eccentric groove, and long adcarinal ridges that form ventral extensions parallel to the carina (Barrick et al. 2008). The dextral elements of *I. eudoraensis* are similar to the dextral elements of *I. simulator,* but can be distinguished from each other by the ventral extension of the adcarinal ridges. Barrick et al. (2008) assigned *S. luganicus* to *Idiognathodus* and suggested that *I. luganicus* may appear in younger strata than *I. simulator.* Barrick et al. (2008) claimed that a deflected carina is not a species-level character, and stated that the specimens of *S. luosuensis* illustrated by Wang and Qi (2003) have ventral extensions parallel to the carina and appear similar in appearance to *I. luganicus.*

Chernykh (2012) later described two more species from the southern Urals. *Streptognathodus gravis* differs from

S. auritus by having better developed lobes and no rostral ridge flaring. *Streptognathodus postsimulator* is a lobeless form with a strongly angled eccentric groove, and a broader platform than *S. luganicus*.

Geological setting

During Late Pennsylvanian time the Midcontinent sea of North America, and the Russian platform of Eurasia were separated by the large northern landmass of Protopangea and were connected only by a narrow northern seaway during periods of global sea-level highstands (Fig. 1A). During these periods of highstand, the Midcontinent sea of North America extended from the Appalachian highlands in the south, to the ancestral Rocky Mountains and, in places, connected to the Protopacific ocean "Panthalassa" to the west and northwest (Fig. 1B). Late Pennsylvanian deposition in the Midcontinent Basin was controlled by glacial-eustatic sea level rise and fall, which created repetitive and cyclic stratigraphic sequences "cyclothems" throughout the region (Heckel 1994, 1999). The Oread is a major cyclothem and contains in ascending order, the upper portion of the Snyderville Shale, the Leavenworth Limestone, the Heebner Shale, the Plattsmouth Limestone, and the lower part of the Heumader Shale of the Oread Formation of the Shawnee Group (Heckel 1999). The upper Snyderville Shale that occurs above a thin carbonate lag is interpreted as a transgressive fossiliferous shale and marks the beginning of the Oread cyclothem. The Leavenworth Limestone is the transgressive limestone of the cycle and is abruptly overlain by the Heebner Shale (Fig. 2A). The maximum transgressive surface of this megacycle occurs within the Heebner Shale. The Plattsmouth Limestone overlies the Heebner Shale and is the regressive limestone of the cyclothem. This limestone contains a diverse fauna of fusulinids, corals, bryozoans, crinoids and abundant phylloid algae that create wavy, algae-laminated bedding surfaces. The regression is interpreted to continue up section into the lower Heumader Shale, which represents marginal marine deposition and the end to the Oread cyclothem (Boardman 1999).

The Heebner Shale is 140 cm thick at the I-229 roadcut, 155 cm thick at Clinton Dam and 190 cm thick at the Old Sedan spillway (Fig. 2B). The lower 5 cm of each section is gray shale containing abundant brachiopods. The overlying black shale at the Sedan and Clinton sections is subdivided into two parts. The lower half is composed of dark fissile shale and the upper half is black fissile shale with intervals of phosphate concretions. These concretions form laterally continuous beds at Sedan, but are more randomly distributed at Clinton. A 3-cm-thick, laterally continuous and resistant bed of coarse phosphatic sand was observed only at Clinton. *Ammodiscus*, *Planolites*, and occasionally fish debris can be found in the black shale. The black shale at all three sections grades up into a gray shale that contains productid brachiopods, bryozoans, crinoids, and low-spired
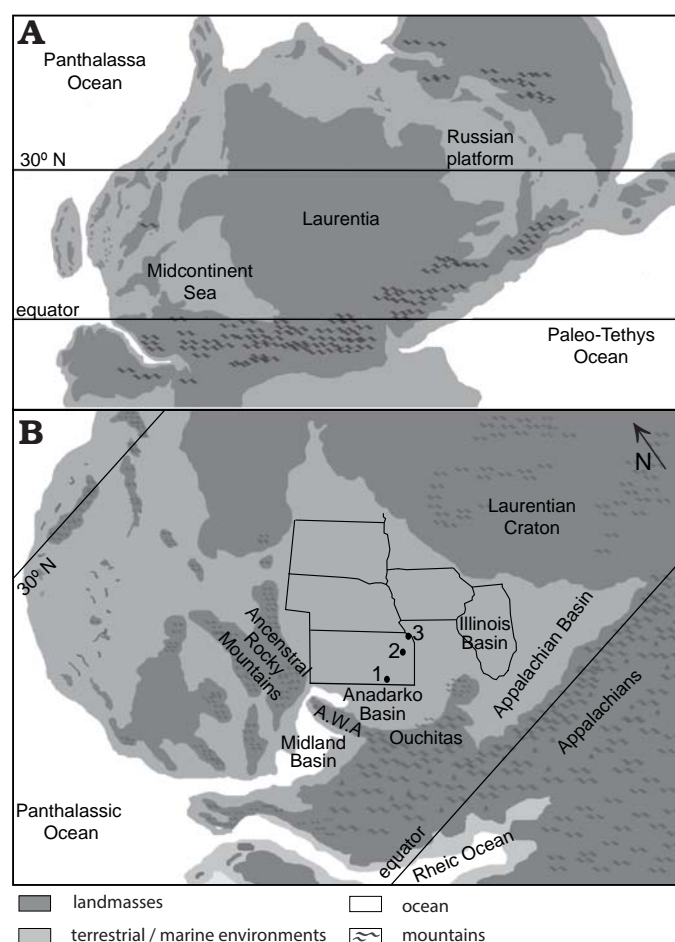

Fig. 1. Paleogeographic map of Laurentia (**A**) and the Midcontinent sea (**B**) during Late Pennsylvanian time. Terrestrial/marine environments represent regions dependent on glacio-eustatic and basin controls. Modern day state outlines for reference to sample locations: 1, Sedan spillway; 2, Clinton Dam; 3, interstate I-229 roadcut. A.W.A., Ancestral-Wichita-Amarillo mountains. A, based on Heckel (1999); B, modified from Algeo and Heckel (2008).

gastropods. The gray shale is most calcareous at the top and begins to form partially cemented beds just below the contact with the Plattsmouth Limestone.

Material and methods

Conodont samples.—The Heebner Shale was sampled at five-centimeter intervals at three different locations within the Midcontinent region (Figs. 1B, 2B; Appendix 1). The northernmost of these outcrops is along interstate I-229 northwest of St. Joseph in Andrew County, Missouri. A central section is located at the Clinton Dam spillway just southwest of Lawrence in Douglass County, Kansas. The southernmost location is the old Sedan City Lake spillway in Chautauqua County, Kansas. (Fig. 1B; Appendix 1). All measurements in the following descriptions are taken upward from the contact between the base of the Heebner Shale and the top of the underlying Leavenworth Limestone.
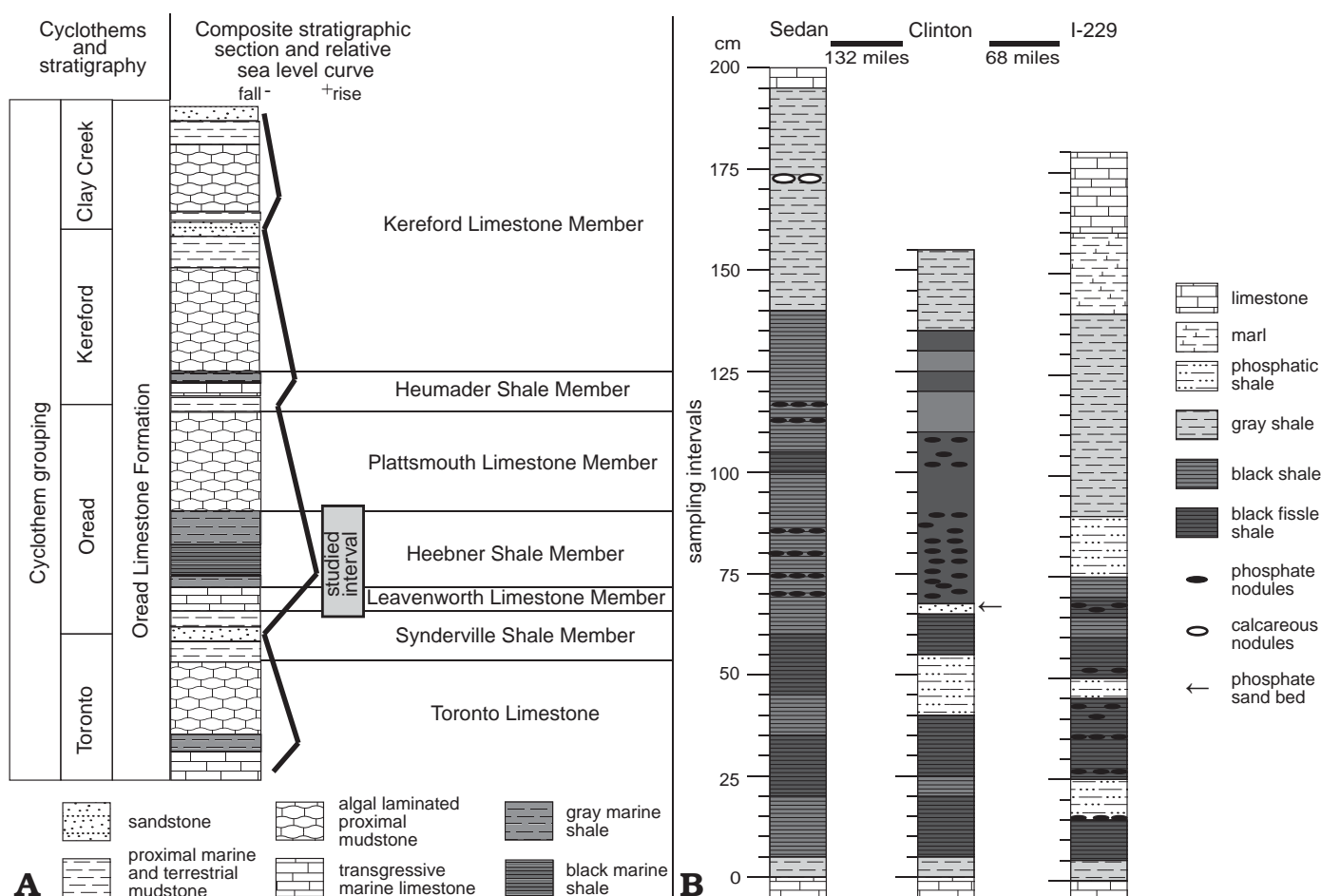
Fig. 2. **A**. Composite stratigraphic section of the lithologic members of the Oread Megacylothem and relative sea level curve; modified from Heckel (1999, 2013). **B**. Detailed measured stratigraphic sections of the Heebner Shale at each locality. Darkness of the shale intervals corresponds to the darkness of the shale in hand sample. See SOM 1 for exact locations.

Gray shale samples were dried and then submerged in kerosene for approximately 4 to 5 hours to aid in the deflocculation of the clay grains. The kerosene was poured off, and the sample was submerged in hot water and allowed to sit overnight in order to thoroughly disaggregate the sample. Black shale samples were submerged in a 12% bleach solution (sodium hypochlorite) in order to break down the organic material. The solution was poured off and replaced every month until the shale began to lighten in color and break down into a fine residue. This process can take several months depending on the amount of organic material in the sample. Once the organics had been destroyed, the sample underwent the gray shale procedure. Limestone samples were crushed into small (1–3 cm diameter) pieces and dissolved in a 10% buffered formic acid solution to dissolve carbonate material. Samples were sieved to a small size (120 μm). When necessary, the residues were placed in heavy liquids for density separation.

Several thousand P_1 elements of *Idiognathodus* were collected from the Heebner Shale at the three outcrop localities. *Idiognathodus* specimens that possessed an eccentric groove were classified as belonging to the *I. simulator* group and specimens that lacked an eccentric groove were

classified as belonging to either the *I. tersus* (Ellison 1941) or *I. pictus* groups (Chernykh 2005) (for details see SOM 1: tables 2, 4, 6; Supplementary Online Material available at http://app.pan.pl/SOM/app61-Hogancamp_etal_SOM.pdf). Many P_1 elements of *Idiognathodus* were split in half along the eccentric groove, a breakage habit described by Von Bitter (1972). If a P_1 element was complete from the dorsal termination of the carina to the dorsal tip it was counted as the appropriate species. If the element met this criterion but breakage prevented conclusive identification of the specimen as one of a specific species then it was tabulated as an *Idiognathodus* or *Streptognathodus* P_1 element. Only every other split P_1 element was counted. Sinistral and dextral P_1 elements were counted separately to ascertain which dextral and sinistral morphotypes tend to occur together.

While picking specimens from residues, it was observed that all very small specimens lacked lobes and appeared nearly identical in morphology. Because juvenile specimens of many different animal species may appear identical early in their ontogenetic sequence, a size minimum had to be established before picking specimens for morphometric analysis. A minimum length of approximately 0.3 to 0.4 mm from the ventral tips of the adcarinal ridges to the dorsal tip was selected as the

minimum size to evaluate lobe development. This means that the earliest ontogentic stage of these species is excluded from the subsequent analyses, but this omission allows for a more accurate comparison between adult morphologies.

Geometric morphometrics procedures.—Morphometrics is the quantitative study of shape and form. Traditional morphometrics involves taking measurements of lengths, widths, angles, areas, ratios and other similar properties. These measurements are often made on particular features that the investigator might interpret as being homologous. It is important to note that any morphological information that is not measured is lost to the analysis. In contrast, geometric morphometrics focuses on the spatial relationships among anatomical "landmarks" (typically points marking the boundaries between abutting structures) and takes into account the geometric relationships of every landmark with every other landmark. More thorough discussions of the comparisons between traditional morphometrics and geometric morphometrics can be found in Rohlf (1990), Rohlf and Marcus (1993), and Adams et al. (2004). Various types of landmarks can be used, including ones that are not necessarily tied to truly homologous features. Because conodonts can have "plastic" features, dramatic ontogenetic change, a wide array of ornamentation, and are often discriminated on a basis of shape and features rather than size, geometric morphometrics is an ideal approach for characterizing their morphological features. Additionally, many conodont species have unique sets of shapes and characters that lend themselves toward the development of landmark-based analyses.

P_1 elements were photographed at an orientation such that the denticles of the carina were parallel to the angle of the camera. For the morphometric analysis of the *Idiognathodus simulator* group, 263 elements were included in the analyses. Photographs for morphometric analysis were all taken on the Nikon SMZ1500 using the same camera, file and magnification settings. JPEG files were converted to TPS format using the software TpsUtil (Rholf 2010a). Landmarks were digitized on the TPS files using the software TpsDig (Rholf 2010b). Multivariate analyses were performed and wireframe images were generated using the software MorphoJ (Klingenberg 2011) as described in the following sections (see SOM 2 for morphometric data).

Step 1. Landmark definitions: Bookstein (1991) defines three different categories of landmarks. Type 1 landmarks are interpreted as being truly homologous points between all specimens. Type 2 landmarks are points that can be defined and located on all specimens, but may or may not be truly homologous points. Type 2 landmarks are often used as helping points, or sliding landmarks along a boundary formed between Type 1 landmarks. Lastly, Type 3 landmarks are defined by measures of extremity such as end points of maximum length or width, and do not need to be placed along a homologous boundary. Further discussion and examples of the process of defining and digitizing landmarks can be found in Zelditch et al. (2004).
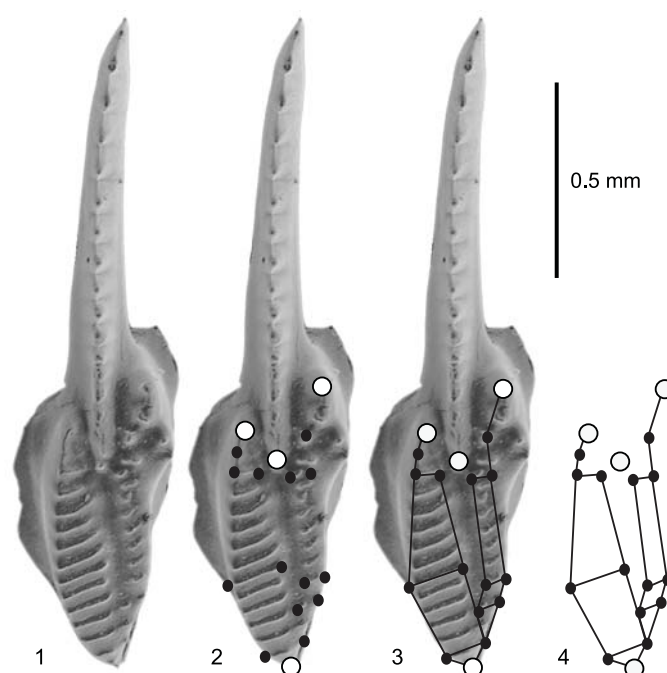

Fig. 3. Transformation of a conodont P1 element into morphometric coordinate points: 1, specimen is photographed; 2, coordinates are placed on the image using the software TspUtil; 3, wireframe outline is created by linking landmarks to each other; 4, image is removed to illustrate that all analyses beyond this point are performed on the landmarks only, and all other biological criteria are no longer considered. Open circles, location of Type 1 landmarks, and black ovals, location of Type 2 landmarks.

Four Type 1 landmarks and fourteen Type 2 landmarks were defined on the P_1 elements of the *Idiognathodus simulator* group using Bookstein's (1991) landmark definitions, resulting in a total of 18 landmarks for analysis (Figs. 3, 4). Dextral images were mirrored prior to landmark placement to allow specimens to be analyzed with natural chirality orientation effects removed. The numbers listed after the anatomical features in the following sentences reference the landmark numbers in Fig. 4, and the anatomical features defined in SOM 3. The Type 1 landmarks are the dorsal tip of the element (16), the dorsal termination of the carina (2), and the ventral terminations of the adcarinal ridges (1, 3). The Type 2 landmarks are the midpoints along the adcarinal ridges (17, 18), the rostral and caudal terminations of the most ventral and most dorsal transverse ridges (4–7, 12–15), and the rostral and caudal terminations of the transverse ridges nearest the point of maximum curvature along the caudal and rostral platform margins (8–11).

Step 2. Definitions of groups for morphometric analysis: Specimens from the *Idiognathodus simulator* group were assigned membership to a number of qualitative groups. Groups were chosen to focus on anatomical features that have been used in the previous species discrimination of *Idiognathodus*. These groups included categories defined by chirality, groove, lobes, geographic location, and a series of morphotype groups. Chirality membership was either sinistral or dextral. Lobe group membership was divided into four categories, 0 lobes, 1 lobe, 2 lobes, or a discon-
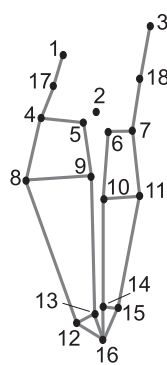
Fig. 4. Wireframe created by connecting landmarks chosen for the *Idiognathodus simulator* morphometric analysis. Numbers represent the landmark number designations used for the morphometric analysis: 1, ventral termination of the rostral adcarinal ridge; 2, dorsal termination of the carina; 3, ventral termination of the caudal adcarinal ridge; 4, rostral termination of the most ventral transverse ridge on the rostral side; 5, caudal termination of the most ventral transverse ridge on the rostral side; 6, rostral termination of the most ventral transverse ridge on the caudal side; 7, caudal termination of the most ventral transverse ridge on the caudal side; 8, rostral termination of the transverse ridge closest to the point of maximum curvature along the rostral platform margin on the rostral side. 9, caudal termination of the transverse ridge closest to the point of maximum curvature along the rostral platform margin on the rostral side; 10, rostral termination of the transverse ridge closest to the point of maximum curvature along the caudal platform margin on the caudal side; 11, caudal termination of the transverse ridge closest to the point of maximum curvature along the caudal platform margin on the caudal side; 12, rostral termination of the most dorsal transverse ridge on the rostral side; 13, caudal termination of the most dorsal transverse ridge on the rostral side; 14, rostral termination of the most dorsal transverse ridge on the caudal side; 15, caudal termination of the most dorsal transverse ridge on the caudal side; 16, dorsal tip of the element; 17, midpoint along the rostral adcarinal ridge; 18, midpoint along the caudal adcarinal ridge.

nected adcarinal ridge. Location group was one of the three stratigraphic sections, Clinton, Sedan, and I-229. Specimens with more than two truncated longitudinal transverse ridges were classified as grooved, and those with two or fewer truncated transverse ridges were classified as non-grooved. The term "incomplete" was used to designate specimens that had over half of their transverse ridges completed, but still were classified as grooved based on the two ridge criterion. In the morphometric analyses these "incomplete" specimens were included as "grooved" to maintain purity of the "grooveless" classifier.

Morphotype membership for the *Idiognathodus simulator* group was determined on the basis of element shape, presence of an eccentric groove and lobe group membership. These criteria were chosen because these features are typically used for the discrimination of *Idiognathodus* species. Nearly all specimens could be confidently categorized as one of five morphotypes that have an eccentric groove. *Idiognathodus luganicus* (Kozitskaya 1978) has no lobes. *Idiognathodus lateralis* sp. nov. and *I. praenuntius* (Chernykh 2005) have one caudal lobe. *Idiognathodus praenuntius* is distinguished from *I. lateralis* sp. nov. by the higher degree of symmetry between the platform margins and a more medial position of the eccentric groove.

Idiognathodus auritus (Chernykh 2005) has both caudal and rostral lobes. *Idiognathodus simulator* (Ellison 1941) has a caudal adcarinal ridge that is separated from the caudal platform margin by the caudal adcarinal trough.

Step 3. Procrustes superimposition: A generalized Procrustes superimposition procedure translates, scales and rotates all specimens to their best mutual fit, and is used to remove the shape bias affiliated with specimen size, image position and rotation. The centroid size is defined as the square root of the summed Euclidean distances from each landmark to the specimen centroid. All specimen centroids are centered, and then all individuals are scaled to a common centroid size and rotated to a best fit. A "best fit" composite represents the shape created when using the mean values for each landmark (i.e., the landmark centroids) and essentially provides an "average" shape for the data set. Results from the Procrustes analysis were compared with results from a resistant-fit theta-rho analysis (RFTRA) to validate the assumption of landmark homogeneity in the Procrustes analysis. Getting similar results for both analyses informs

the investigator that no one single landmark is overwhelmingly variable and effecting the location of other landmarks. Procrustes analysis is an important preliminary step because once the shape, scaling, and orientation noise is removed, the only variation that should remain between specimens is their true shape variation. In summary, this procedure provides an average shape reconstruction for the data set, and this information is required for the subsequent procedures and analyses. Application and theory of superimposition techniques are summarized by Zelditch et al. (2004), and are discussed in more mathematical detail in Rohlf and Slice (1990).

Step 4. Generating a covariance matrix: A covariance matrix can be generated after performing a Procrustes analysis. This is accomplished by calculating the sums of square roots and cross products (SSCP) of the deviations from the column means, which are the Procrustes coordinates (the landmark coordinates associated with the average shape; the landmark centroids), and the deviations would be the SSCP's of the deviations in the X and Y coordinates between an individual specimen and the Procrustes coordinates. These values can be used to compare individuals with the mean form calculated from the Procrustes analysis. The importance of this step is that for each specimen the raw coordinate values have been replaced with the deviations from the "mean" shape calculated from the Procrustes analysis, thus constructing a new data matrix that only contains values pertaining to variation in shape.

Step 5. Eigen analyses: Eigen analyses are statistical analyses that use vector geometry to determine the magnitude and direction of co-linear variation in multi-dimensional space. Eigenvectors and eigenvalues are calculated from either a covariance or a correlation matrix. The eigenvector is the vector used to determine the direction of maximum linear variation, and the corresponding eigenvalue is the amount of variance represented by the eigenvector. There will be as many eigenvectors present as there are statistical dimensions available, i.e., the rank of the matrix. The first eigenvector is the vector that best fits the linear variation between all the data in multidimensional space, and it has the largest eigenvalue. The second eigenvector is the vector that best fits the variation not accounted for by the first. Each successive eigenvector represents variation not accounted by the previous eigenvectors. This means that these eigenvectors are mutually orthogonal, have a hierarchy

of significance, and when summed together describe 100% of the original data. No information is lost in these analyses and because of their statistical properties it is possible to deconstruct, dissect, or reconstruct the original matrix.

The two eigen analyses used for morphometric analysis in this study are principal component analysis (PCA) and canonical variate analysis (CVA). Principal component analysis (PCA) is an eigen analysis that calculates the linear variation within a data set under the assumption that all specimens belong to a single group. PCA provides composite variables that best represent the variation among all specimens in the original matrix. A canonical variate analysis (CVA) is an eigen analysis similar to PCA, but differing in that CVA is a discriminatory analysis that calculates the linear variation that best discriminates between multiple groups of variables, whereas PCA assumes all specimens belong to the same group and then describes the linear variation within that group. CVA requires group membership to be determined prior to analysis and assumes that group membership was correctly predetermined for the analysis. The number of eigenvectors for a CVA is dependent on the number of groups, and the independence, or mutual orthogonality, of those groups. For example, if a CVA is calculated for two independent groups there will only be one eigenvector representing the linear direction of the most discrimination between the groups in multi-dimensional space. There will always be one less eigenvector than there are number of independent groups. Further information and examples of eigen analyses being used for morphometric studies can be found in Douglas et al. (2001), Depecker et al. (2006), and Strauss (2010).

Step 6. Using eigenvectors to interpret morphological variation: Eigenvectors are calculated from the covariance matrix and are used in both the principal component analysis and canonical variate analysis. These vectors are typically called principal components (PC's) when used in a principal component analysis or canonical variates (CV's) when used in a canonical variate analysis. Each landmark coordinate for each specimen has a scaling for every eigenvector, and each individual specimen has a single score for each eigenvector. The eigenvector score for each specimen is calculated by taking the sum of the products from each raw landmark coordinate multiplied its respective eigenvector scaling. For example, the PC1 score for specimen A would be the sum of the products of each raw landmark coordinate multiplied by its respective PC1 scaling:

$$(X_{1i} \cdot \alpha_{11} X_{1i} + Y_{1i} \cdot \alpha_{11} Y_{1i} + X_{2i} \cdot \alpha_{21} X_{2i} + Y_{2i} \cdot \alpha_{21} Y_{2i} \ldots) = PC1$$

score for an individual, where X_{1i} is the raw coordinate for landmark 1 for specimen i and α_1 is the corresponding principal component scaling coefficient for landmark 1 on PC1. These scores relate to the location of each specimen in multidimensional space relative to the position of the eigenvectors. Because every specimen has a score for every eigenvector, it is possible to create two-dimensional cross plots using any two eigenvectors and the specimen scores for those vectors. This provides the user the ability to create

a two-dimensional window into a multidimensional space. These two-dimensional cross plots are used in the upcoming section to aid in the description and illustration of the distribution of individuals in a multi-dimensional morphospace.

Because the eigenvectors relate to the original data it is also possible to model what a shape would look like by using scores of a chosen PC or CV. Any PC or CV values of zero will result in a landmark configuration that is identical to the average shape created by the Procrustes analysis. Changing the PC or CV value will result in the landmarks shifting from their original positions, and the direction and magnitude of that change is dependent on the PC or CV landmark coordinate scalings for that particular eigenvector. This allows the user to see the spatial change between landmarks as they change in their PC or CV values along a specific eigenvector. This can be used to determine what morphological changes occur along each eigenvector. For example, if negative values of PC1 resulted in a narrow platform element, than positive values of PC1 would result in a wider platform element and we can conclude that change along the PC1 vector corresponds to changes in platform width. This method is used to create wireframe models that illustrate what a theoretical form would look like at a particular location on any chosen eigenvector. These wireframes are included with the two-dimensional PC and CV cross plot figures discussed in the upcoming section and are used to help determine what morphological changes in the P_1 elements correspond with variation along a particular PC or CV eigenvector.

Results

Chirality shape variation.—Principal component analysis of specimens of the *Idiognathodus simulator* group resulted in 32 principal components (PC's) with the first two PC's representing 62.3% of the total variance (Fig. 5). Shape variation along PC1 corresponds with the ventral-dorsal shifting of the point of maximum curvature on the rostral platform margin, the most dorsal transverse ridges along both platform margins, and changes in length of both adcarinal ridges. Shape variation along PC2 corresponds with the inverse ventral-dorsal shifting of the points of maximum curvature on the platform margins, the caudal-rostral shifting of the dorsal tip of the element, and variation in adcarinal ridge length.

When the specimens are coded based on chirality, it is apparent that the sinistral and dextral elements occupy separate regions of morphospace (Fig. 5). To investigate this segregation, a canonical variate analysis was executed using chirality as the classification criterion. This analysis showed a very strong separation between sinistral and dextral elements with nearly no overlapping CV values between sinistral and dextral elements (Fig. 6). The canonical variate analysis shows that the dextral elements have shorter adcarinal ridges, and a more ventral location of maximum curvature along the rostral platform margin, resulting in a more triangular-shaped platform for dextral elements,
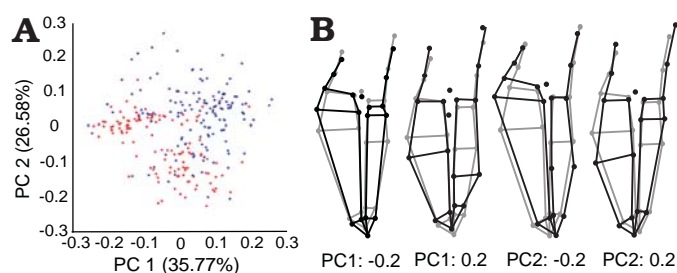
Fig. 5. Principal component (PC) cross-plot and wireframes for all grooved specimens. **A**. Principal component cross plot of the first two principal components, labeled with their corresponding eigenvalues (blue, sinistral; red dextral). **B**. Black wireframes, the resulting form with values of the corresponding principal component values; gray outline, the mean form provided by the preliminary Procrustes fit.
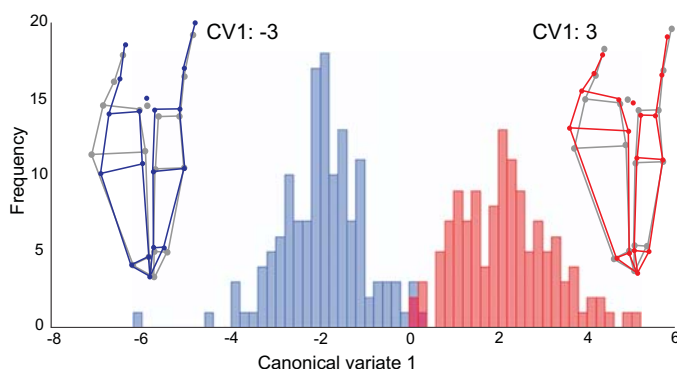

Fig. 6. Canonical variation plot and wireframes for all grooved specimens, using chirality membership as the group-defining criterion. Gray wireframe, the mean form provided by the preliminary Procrustes fit, and blue/red wireframes, form achieved with values of the corresponding canonical variate; blue, sinistral; red dextral.

and a more elongate diamond-shaped platform for sinistral elements. The relative size variation between the rostral platform region and the caudal platform region also tends to be much greater in dextral elements. The segregation between sinistral and dextral elements on the principal component cross-plot indicates that the shape variation associated with chirality membership is the greatest shape variation in the data set. This shows that the shape difference between sinistral and dextral elements will overwhelm any variation associated with other characters in a principal component analysis. Because of this chirality bias, sinistral and dextral elements are analyzed separately in the following analyses of shapes associated with lobe group membership.

Lobe group shape variation.—In order to investigate the shape variation associated with lobe group membership, shape variation associated with chirality asymmetry was removed by performing separate canonical variance analyses for sinistral and dextral elements. Crossplots of the three canonical variates showed a gradational separation of lobe groups in two-dimensional morphospace for sinistral elements (Fig. 7A). The lobeless (*Idiognathodus luganicus*) and disconnected ridge (*I. simulator*) morphotypes are primarily constrained to negative values of CV1, whereas the two-lobed morphotype (*I. auritus*) is confined to positive

values of CV1. The one-lobed morphotypes (*I. praenuntius* and *I. lateralis* sp. nov.) fill the morphospace between them, falling between CV1 values of -2 and 2. The lobeless (*I. luganicus*) and disconnected ridge morphotypes (*I. simulator*) are moderately separated along CV2 and are separated further along CV3. Variation along CV1 corresponds to constriction and expansion of the adcarinal ridge midpoints. Variation along CV2 corresponds with caudal shifting of both adcarinal ridges and some ventral-dorsal shifting of the point of maximum curvature on the rostral platform margin. Variation along CV3 corresponds with change in the orientation of the adcarinal ridges. Positive values of CV3 correspond with a caudally oblique orientation for both adcarinal ridges and negative values of CV3 correspond with adcarinal ridges that are sub-parallel to the platform margins.

Canonical variate analysis of the lobe groups within dextral elements also shows segregation of groups in morphological space (Fig. 7B). Note that the two-lobe character state (*Idiognathodus auritus*) is very rare in dextral elements and has meager representation in the analysis. The crossplot of the first two canonical variates (82.2% of the total variance) shows a gradational segregation between the one-lobe morphotypes (*I. praenuntius* and *I. lateralis*) and all other groups along the CV1 axis. A separation exists between the lobeless (*I. luganicus*) and disconnected-ridge (*I. simulator*) morphotypes along the CV2 axis. Positive values of CV1 show a strong concavity along the caudal edge of the element that spans from the curvature maxima of the caudal platform margin to the ventral tip of the adcarinal ridge. This constriction is also present on the sinistral elements. However, in the sinistral elements the constriction did not extend as far along the platform margin. Variation along CV1 corresponds with concavity of the caudal edge of the element, caudal-rostral shifting of the dorsal tip, as well as obliquity changes and the dorsal-ventral shifting of the rostral transverse ridges. CV2 values also vary with the concavity of the caudal edge and the flaring of the rostral adcarinal ridge. The cross plot of CV1 and CV3 (~68% of the total variance; Fig. 7B) shows weak separation between groups suggesting that most of the separation between specimens in morphospace occurs along CV1 and CV2.

The adcarinal ridges appear to constrict with the presence of lobe growth on all specimens. Dextral elements experience much more dorsally-ventrally extensive platform margin constriction and adcarinal ridge concavity in the presence of lobe growth. Specimens with disconnected adcarinal ridges (*Idiognathodus simulator*), for both sinistral and dextral elements, show that the midpoint of the adcarinal ridge flares outward from the carina.

Morphotype shape variation.—*Idiognathodus luganicus* has an eccentric groove and no lobe development. A crossplot of the first two principal components reveals some separation in morphospace between sinistral and dextral elements, with dextral elements falling in the lower left half of the graph, and sinistral elements in the upper right portion (Fig. 8A).
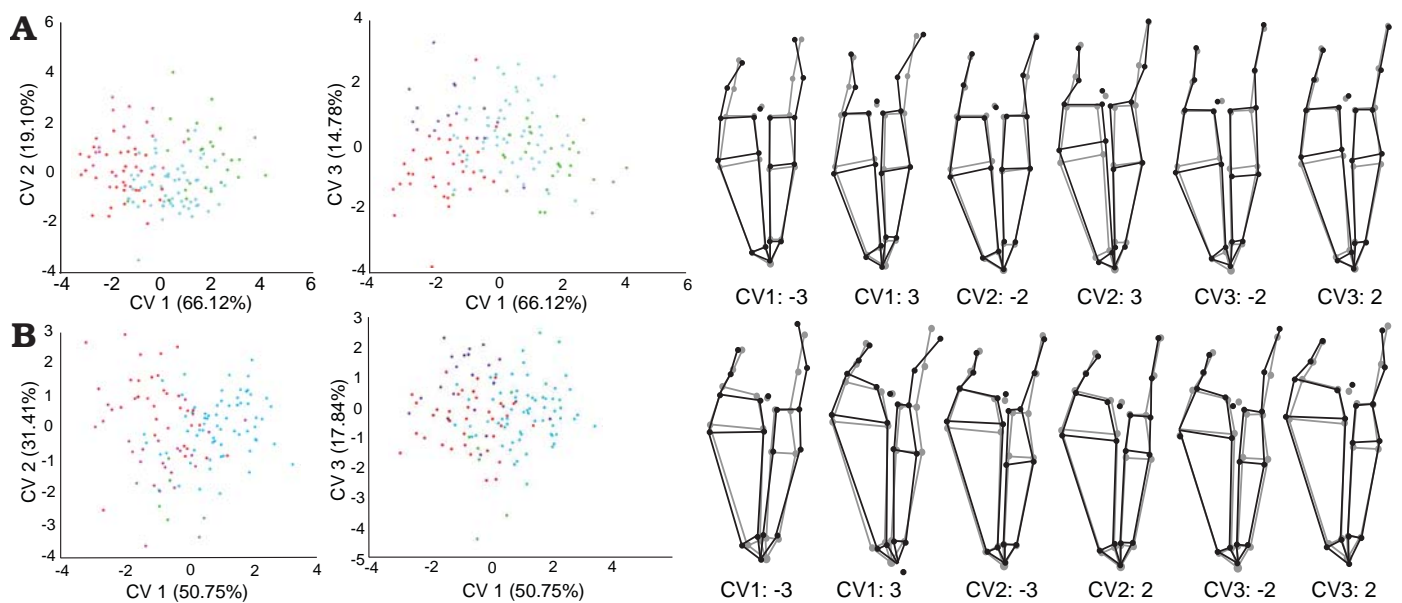
Fig. 7. Canonical variation (CV) cross-plots and wireframes for all grooved sinistral (**A**) and dextral (**B**) elements, using lobe membership (red, 0 lobes; blue, 1 lobe; green, 2 lobes; purple, dicconnected ridge) as the group-defining criterion. Gray wireframes, mean form provided by the preliminary Procrustes fit; black wireframes, form achieved with values of the corresponding canonical variate.

A canonical variate analysis supports this shape distinction between sinistral and dextral elements (Fig. 8B). Sinistral elements have relatively straight platform margins, with the locations of maximum curvature in a medial position along both margins. However, the rostral margin extends farther laterally than the caudal margin. The rostral adcarinal ridge is slanted toward the carina, and the caudal adcarinal ridge tends to extend sub-parallel to the carina and the caudal platform margin, giving the element a relatively straight caudal edge and a broad, gradually curved rostral edge. The dorsal termination of the carina is typically ventral of the most ventral transverse ridges. Dextral elements also exhibit a relatively straight caudal element edge, sub-parallel to the carina, but differ from the sinistral elements primarily owing to shape variation on the rostral platform margins. The point of maximum curvature along the rostral platform margin is typically located in a more ventral position on the dextral elements, usually near the most ventral ridge. The most ventral ridge on the rostral side of dextral elements is located in a more ventral position than in the sinistral elements, and frequently lies beyond the dorsal termination of the carina. The ventral extension of the rostral platform region and the point of maximum curvature result in a wide ventral region that tapers dorsally. This wide ventral region is also associated with a steep deflection of the rostral adcarinal ridge toward the carina.

Idiognathodus lateralis sp. nov. has an eccentric groove and a caudal lobe. A crossplot of the first two principal components and a canonical variate analysis of chirality reveal that this morphotype contains asymmetrical dextral and sinistral elements (Fig. 9A, C). Both sinistral and dextral elements have slightly concave caudal adcarinal ridges and ventral platform margins. The maximum curvature of the rostral platform margin is shifted farther ventrally in the dextral ele-

Fig. 8. Cross-plot of the first two principal components (labeled with their corresponding eigenvalues) and wireframes (**A**) and canonical variation plot (using chirality membership as the group defining criterion) and wireframes (**B**) for *Idiognathodus luganicus*. Black wireframes, form with values of the corresponding principal component values; gray wireframes, mean form provided by the preliminary Procrustes fit; blue/red wireframes, form achieved with values of the corresponding canonical variate; blue, sinistral; red, dextral.

ments than the sinistral elements and gives the rostral margin a sharper, more triangular edge. This change in the rostral platform region is the source of the most variation between the sinistral and dextral elements and comprises much of the variation along the PC2 axis. Both sinistral and dextral elements vary in the location of maximum curvature along their
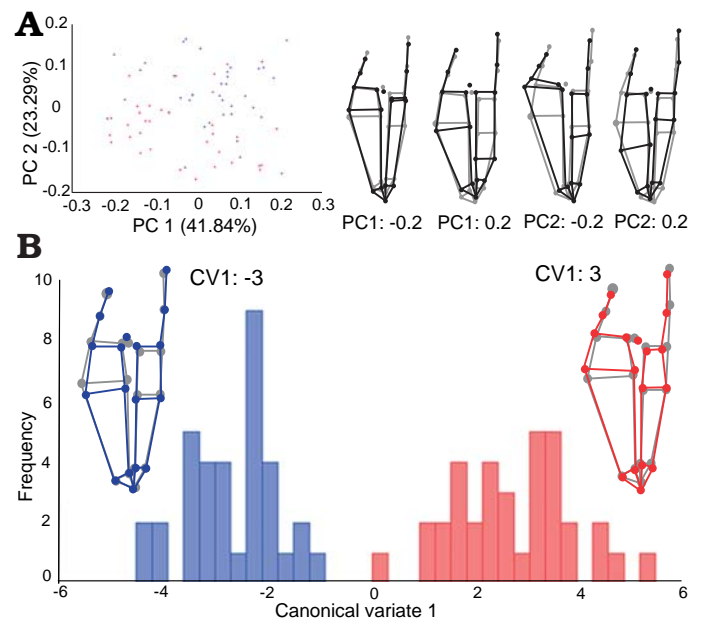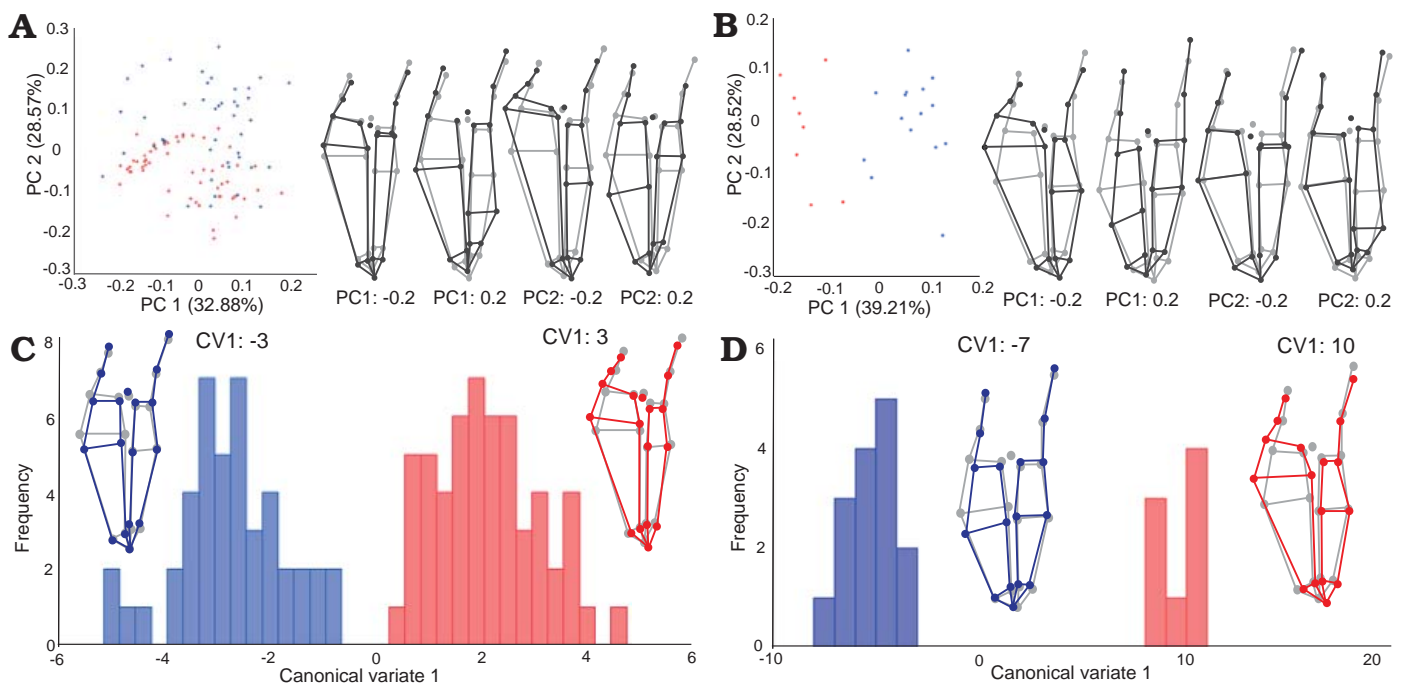
Fig. 9. Principal component cross-plots of the first two principal components (labeled with their corresponding eigenvalues) and wireframes (A, B) and canonical variation plots (using chirality membership as the group defining criterion) and wireframes (C, D) for *Idiognathodus lateralis* (**A**, **C**) and *Idiognathodus praenuntius* (**B**, **D**). Black wireframes, form with values of the corresponding principal component values; gray wireframes, mean form provided by the preliminary Procrustes fit; blue/red wireframes, form achieved with values of the corresponding canonical variate; blue, sinistral; red, dextral.

caudal platform margins. Both adcarinal ridges flare caudally for sinistral and dextral elements, but the group shows variation in the angle of deflection. The rostral platform region is larger than the caudal platform region. However, in some dextral elements the most ventral ridge on the rostral side is located ventral to the dorsal termination of the carina, similar to the dextral elements of *I. luganicus*.

Idiognathodus praenuntius has an eccentric groove and a caudal lobe, but is distinguished from *I. lateralis* sp. nov. by having a more medial location of the eccentric groove, and more symmetrical platform margins. This morphotype exhibits asymmetrical pairs, as shown by the results of the principal component analysis and a canonical variate analysis (Fig. 9B, D). A broader rostral platform margin with a ventrally shifted point of maximum curvature is characteristic of the dextral elements and is the major difference between the sinistral and dextral elements. The relative length of the platform is typically shorter for both sinistral and dextral elements of this morphotype and the adcarinal ridges tend to maintain a sub-parallel orientation to the carina, although some elements, primarily dextral elements, may flare caudally. The caudal platform margin tends to have a much more dorsal location of maximum curvature than other morphotypes, giving these specimens a more symmetrical and elliptical platform shape.

Specimens having an adcarinal ridge disconnected from the platform margin by the adcarinal trough are *Idiognathodus simulator*. In some larger specimens of *I. simulator*, a small lobe is developed on the rostral margin, but these specimens were not placed in *I. auritus*, ow-

ing to the disconnected adcarinal ridge on the caudal side. Principal component analysis suggests shape variation between the sinistral and dextral elements (Fig. 10A), and a canonical variate analysis confirmed this (Fig. 10C). The trend of a more ventrally shifted point of curvature maxima along the rostral platform margin is more common in the dextral elements and is the primary shape difference between the sinistral and dextral elements for this morphotype. Another asymmetrical feature of this morphotype is the orientation of the disconnected adcarinal ridge. For sinistral elements this ridge tends to be oriented at a more oblique angle to the carina than in the dextral elements. In most sinistral elements, the ventral part of the caudal platform margin flares rostrally at an angle sub-parallel to the orientation of the disconnected adcarinal ridge. Many dextral elements have a caudal platform margin and a disconnected ridge that maintain a sub-parallel orientation to one another and to the carina. For dextral elements, the curvature maximum is located near the most ventral ridge on the caudal side, and near the platform margin midpoint on the rostral side.

Specimens with an eccentric groove and lobe development on both the rostral and caudal sides are *Idiognathodus auritus*. Dextral forms are rare, but the few dextral elements in this analysis appear to segregate distinctly from the sinistral elements in a principal component analysis (Fig. 10B) as well as in a canonical variate analysis (Fig. 10D). The most distinguishing character between chiralities appears to be the position of maximum curvature along the rostral platform margin, as well as a shortening of the adcarinal ridges in dextral forms. All specimens tend to exhibit concavity of
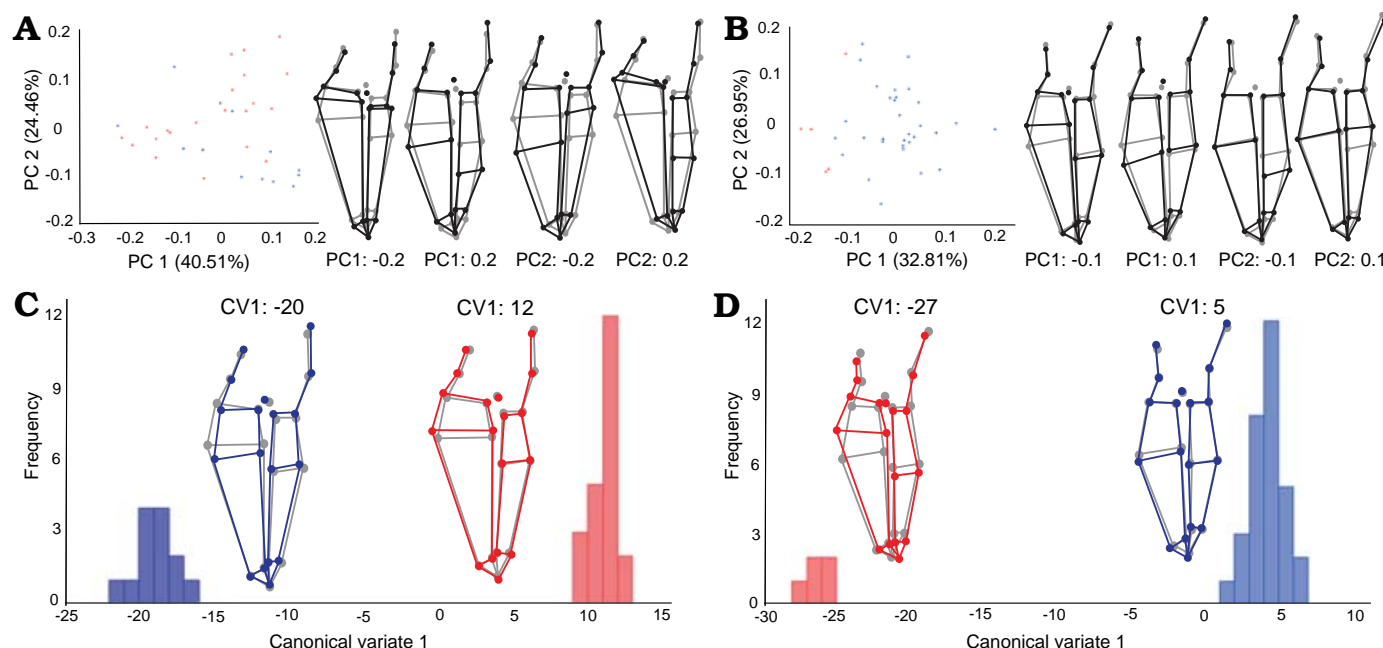
Fig. 10. Principal component cross-plots of the first two principal components (labeled with their corresponding eigenvalues) and wireframes (A, B) and canonical variation plots (using chirality membership as the group defining criterion) and wireframes (C, D) for *Idiognathodus simulator* (**A**, **C**) and *Idiognathodus auritus* (**B**, **D**). Black wireframes, form with values of the corresponding principal component values; gray wireframes, mean form provided by the preliminary Procrustes fit; blue/red wireframes, form achieved with values of the corresponding canonical variate; blue, sinistral; red, dextral.

the ventral portion of the platform margins and the adcarinal ridges, forming a rostrum. Although the dextral elements have the maximum curvature of the rostral platform margin shifted ventrally, most specimens have their maximum curvature at or near mid-length, giving these specimens a platform shape similar to *I. praenuntius*. On the basis of platform shape and the position of the eccentric groove, some of these specimens are similar to those included in *I. praenuntius,* but differ in the presence of a rostral lobe.

In all the shape analyses discussed in previous sections, the size aspect was removed in the preliminary Procrustes analysis. To study allometry, the centroid size calculated from the raw landmark data during the Procrustes analysis was recovered from the data matrix and used as a measure of size. The centroid for each specimen is the center point that minimizes most the total summed distance from each landmark to the centroid. The centroid size is the sum of the square roots of the distances between each landmark to the image centroid. Using this as a measure of size is different than a measurement of length or width, as the lateral expansion of any landmark will increase the centroid size. However, comparison with the photographed specimens indicates that a centroid size of 800–1000 pixel units corresponds to a specimen with a platform length of approximately 0.3–0.4 mm.

A plot for the centroid size of each specimen on the y-axis, and their morphotype membership along the x-axis was created for sinistral and dextral specimens of the *Idiognathodus simulator* group (Fig. 11). At a small size, approximately less than 0.3 mm in platform length, all sinistral and dextral elements of the *I. simulator* group lack lobes, and appear
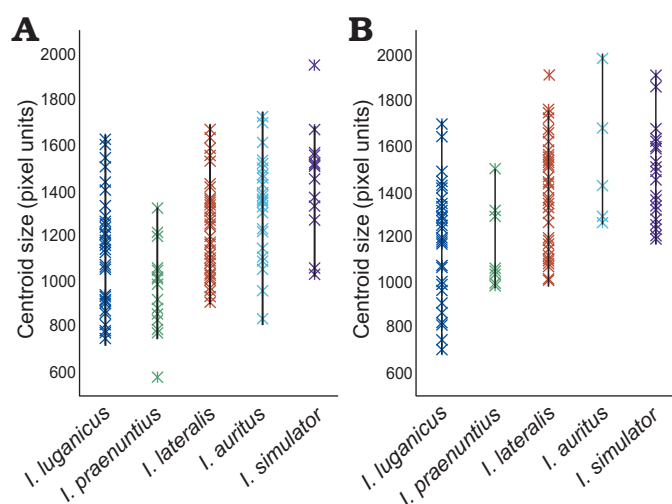
Fig. 11. Cross-plot of morphotype membership for each grooved sinistral (**A**) and dextral (**B**) specimen on the x-axis and their centroid size along the y-axis. Centroid size is not a measure of length, because the outwards movement of any landmark from the centroid will cause it to increase, but for the sake of providing reference, specimens with a platform length less than 0.4 mm generally had a centroid size below 900.

similar to one another. For the sinistral elements, lobes can be distinguished at slightly larger sizes (greater than 0.3 mm platform length), but the presence of two lobes is less apparent at smaller sizes (platform lengths between 0.3 and 0.4 mm). In dextral elements lobes may not develop until a larger size than in sinistral elements. The morphotype *I. simulator* appears to show strong allometric bias in both sinistral and dextral elements, for it cannot be recognized in the smaller specimens.

Morphologic variation by locality.—Species of the *Idiognathodus simulator* group occur through the Heebner Shale in all three sections. The P_1 elements are most abundant in the black fissile shale. In black shale samples from the lower portion of the Heebner Shale, the *I. simulator* group makes up 80 to 90 percent of the conodont elements present, with the remaining portion being composed of *Idioprioniodus* and/or *Streptognathodus* elements (SOM 1: tables 2, 4, and 6). *Idiognathodus luganicus* and *I. lateralis* sp. nov. are the most common morphotypes and *I. simulator* is relatively uncommon. The only member of the *I. simulator* group that shows any stratigraphic or geographic preference is *I. praenuntius*, which appears more commonly in the lower half of the Heebner Shale in all three sections and is nearly absent northward at the I-229 roadcut. Canonical variate analysis by locality was run for both sinistral and dextral P_1 elements of the *Idiognathodus simulator* group. In both analyses locality membership appears to separate into partially distinctive, but moderately overlapping, regions of two-dimensional morphospace (Fig. 12). Sinistral elements vary in adcarinal ridge length and curvature along CV1, as well as in lengthening and shortening of the platform, and thinning or thickening of the platform region caudal of the eccentric groove. Sinistral element shape along the CV2 axis corresponds with adcarinal ridge length as well as a dorsal-ventral shifting of the curvature maxima along both platform margins. CV1 values for dextral elements vary primarily with overall platform narrowing and widening, length changes of the platform and the adcarinal ridges, as well as the curvature of the caudal platform margin, and the direction of caudal adcarinal ridge deflection. Increasing positive values along the CV2 axis indicate longer adcarinal ridges and a dorsal shifting of the curvature maxima on both platform margins, with the

Fig. 12. Canonical variation (CV) cross-plots and wireframes for all grooved sinistral (**A**) and dextral (**B**) elements, using locality (red, Clinton; green, I-229; blue, Sedan) as the group-defining criterion. Gray wireframes, mean form provided by the preliminary Procrustes fit; black wireframes, form achieved with values of the corresponding canonical variate.

opposite holding true for negative CV2 values. The two morphologic features most associated with change in locality are adcarinal ridge and relative platform size variation in both the sinistral and dextral elements. For both elements, the subpopulation from the Sedan locality tends to have longer adcarinal ridges, and shorter, wider platform regions. The I-229 specimens, as a whole, exhibit longer platforms and more oblique transverse ridges.

Discussion

The geometric morphometric analyses of the five morphotypes of the *Idiognathodus simulator* group demonstrate that the sinistral and dextral P_1 elements occur as asymmetrical pairs in each morphotype, despite differences in lobes and platform shape. The dextral elements are typically widest near the ventral end of the platform, giving these elements a more triangular shape than their curved sinistral counterparts. The greater width of the dextral element is due to the lateral expansion of the rostral platform margin during growth. The difference in width between the sinistral and dextral elements increases with size. The degree of asymmetry also increases as the elements increase in size and the dextral elements transform greater from the juvenile morphology than the sinistral elements. Dextral elements show a greater allometric bias for lobe development and adcarinal ridge isolation, which suggests that sinistral elements may prove more useful in diagnosing species membership in smaller specimens.

P_1 element asymmetry is not unknown in *Idiognathodus* and *Streptognathodus* species and has been expressed by different species groups at different times during the Pennsylvanian. *Idiognathodus* species with strong P_1 element asymmetry are known from Bashkirian strata (e.g., *Idiognathodus sinuosus* Ellison and Graves, 1941; see Lane and Straka 1974). However, most Moscovian and Kasimovian species appear to have had more symmetrical, mirror-image P_1 elements. The *I. simulator* group represents the redevelopment of P_1 element asymmetry in one lineage during the late Kasimovian and early Gzhelian (see Systematic palaeontology section), before the extinction of the genus in the Gzhelian. Then, near the end of the Gzhelian and into the Asselian (Early Permian) species of *Streptognathodus* independently developed asymmetrical P_1 element pairs (Boardman et al. 2006).

The five morphotypes distinguished in this study are considered to represent different species that can be distinguished on the presence of caudal and rostral lobes, character of the adcarinal ridges, and platform shape. These are the same features that have been used to distinguish co-occurring species in *Idiognathodus* and *Streptognathodus* (e.g., Boardman et al. 2006; Chernykh 2005, 2012; Rosscoe and Barrick 2009, 2013). The most common species in the Heebner Shale are *I. lateralis* sp. nov. and *I. luganicus*, whereas *I. simulator*, *I. auritus*, and *I. praenuntius* are less
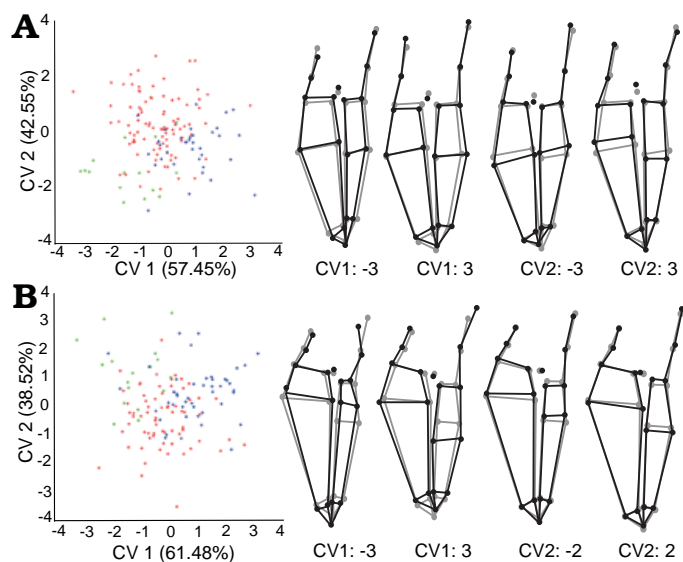
common. All of these species occur throughout the Heebner Shale at all three localities. *Idiognathodus simulator* is not the most abundant species of the *I. simulator* group, but does consistently occur where the *I. simulator* group is present.

Previously, the name *Idiognathodus simulator* was used to designate a large variety of P$_1$ elements that share a caudal lobe and an eccentric groove (Barrick et al. 2008; see Systematic palaeontology section). Based on features of the holotype and the geometric morphological analysis, the concept of *I. simulator* is restricted to only P$_1$ elements with a high, elongate and isolated caudal adcarinal ridge. The adcarinal ridge extends beyond the end of the platform margin into the region where a caudal lobe would be present. The adcarinal ridges and platform margins form the outer platform boundaries of the P$_1$ element and because a lobe is defined as growth outside the boundaries, this feature cannot be classified as a lobe. The new species *I. lateralis* sp. nov. is erected here to designate specimens that have a caudal lobe and a continuous connection between the caudal platform margin and the caudal adcarinal ridge. Discrimination between these two taxa is justified by the morphological differences through most ontogenetic stages of growth. However, at platform sizes smaller than 0.4 or 0.3 mm in maximum length, species of the *I. simulator* group become difficult to distinguish. This is because *I. simulator* has a juvenile state that shows weak separation between the adcarinal ridge and the platform margin. At these sizes it may be difficult to distinguish whether or not the first caudal node is located on a lobe or is protruding out as an extension of the adcarinal ridge. When the platform gets larger than 0.3 or 0.4 mm in length this distinction can be more confidently made. The more precise definition of *I. simulator* should aid in the accurate correlation of the base of the Gzhelian, once a Global Boundary Stratotype Section and Point (GSSP) is chosen (Heckel et al. 2008). This may help avoid the confusion that has arisen recently at other chronostratigraphic boundaries where conodont species were not sufficiently described before the GSSPs were chosen (e.g., *Siphonodella sulcata* for the base of the Carboniferous [Kaiser and Corradini 2011; Corradini et al. 2013]; *Declinognathodus noduliferous* for the base of the Pennsylvanian [Sanz-López et al. 2006; Sanz-López and Blanco-Ferrera 2013]).

Because the Oread cyclothem, which includes the Heebner Shale, represents only a brief interval of time, 100 000 to 400 000 years, related to orbital eccentricity forcing (e.g., Heckel 1986, 2008; Davydov et al. 2010), we cannot resolve the origin of *Idiognathodus simulator* and related species, nor the order in in time in which these species appeared. The Oread cyclothem is a major cyclotherm, one of few Midcontinent cyclothems in the latest Kasimovian and early Gzhelian in which a far offshore, organic-rich black shale developed (Heckel 1999). The underlying cyclothems in the Midcontinent region are minor to intermediate cyclothems that have produced *Streptognathodus*-dominated faunas and rare examples of *Idiognathodus* (Barrick et al. 2013a). It is possible that *I. simulator* may have evolved earlier in time than the Oread cyclothem and that its first occurrence in the Midcontinent region is the result of the major flooding event that produced the cyclothem rather than the speciation event that gave rise to *I. simulator*. The stratigraphic record in other regions (Moscow Basin; Alekseev et al. 2009; southern Urals, Chernykh 2005, 2012) also shows that the *I. simulator* group appears abruptly in these sections, with little evidence for the line of descent from ancestral forms.

The morphometric results strongly support the hypothesis that the growth of lobes correlates with concavity along the platform margins. This concavity occurs along the entire dorsal-ventral extent of the lobe. The maximum concavity occurs near the same point where the lobe is widest. For example, the lobeless species *Idiognathodus luganicus* has the straightest platform margins and adcarinal ridges of all the *Idiognathodus simulator* group species from the Heebner Shale. On the other extreme, the species that exhibit lobe growth on both rostral and caudal sides, such as *I. auritus*, have the most concave and curved platform margins and adcarinal ridges. Additionally, species that only have lobe growth on the caudal side, *I. lateralis* sp. nov., *I. praenuntius*, and *I. simulator* only have platform concavity on the caudal side. The rostral side of these single-lobed species appears relatively straight or convex and is similar to the rostral platform margins of lobeless species. The correlation of increased concavity along the platform margins of specimens with lobes is supported by the results of the lobe-group morphometric analysis for both sinistral and dextral elements of the *I. simulator* group (Fig. 7). All specimens of *Idiognathodus* studied here lack lobes at a small size (platform lengths less than 0.3 mm) and the lobes appear at a larger ontogenetic stage. The platform margin of smaller specimens may be slightly concave or the adcarinal ridge may flare outwards prior to the development of nodes. During this stage a "phantom lobe" is present, which is a growth outside of the platform margin that is of nearly equivalent oral height as the main platform surface, but is not yet ornamented with a single node.

Because lobe size, shape and nodosity are so diverse in many species of *Idiognathodus* and *Streptognathodus* and typically correspond with changes in platform shape, the development of particular lobe and platform architectures may be the result of specialization in the processing of particular prey items (Purnell et al. 2000; Rosscoe and Barrick 2009). Because the lobes are of equivalent oral height as the platform surface, and because the platform surface is interpreted to be the surface in contact with prey items (Purnell and Jones 2012; Jones et al. 2012) they must play a role in the processing of prey items. If this hypothesis is correct, than the continued use of lobe and platform shape characters in taxonomic discrimination is still a valid practice, as it seems reasonable to believe that difference species would have fed on a different selection of prey.

The functional significance of asymmetry in P$_1$ element pairs has been shown to allow interlocking during element occlusion in carminiscaphate elements of *Idiognathodus* (Donoghue and Purnell 1999) and *Gnathodus* (Martínez-Pérez et al. 2014b). However, Martínez-Pérez et al. (2014a)

show that asymmetrical pairs of carminate elements of *Pseudofurnishius murcianus* rigidly interlock and leave little room for element rotation, and do not occlude in the same way as do *Idiognathodus* and *Gnathodus* species. This suggests that different groups of conodonts had unique functional relationships between elements of the apparatus related to different modes of food processing, Accurate quantitative analysis of the shape differences between sinistral and dextral P_1 elements, such as that used here, will be essential for future studies of occlusion or element "matching".

Conclusions

Landmark-based geometric morphometric techniques, combined with multivariate eigen analyses, have allowed for the two dimensional spatial analysis of landmarks on P_1 elements of the conodont genus *Idiognathodus*. These data can be visually represented as wireframes and used to compare quantitative statistical variation to qualitative P_1 element shape variation. Principal component analysis was used to determine variation within a particular group of data and canonical variate analysis was used to determine variation between particular groups of data. The morphometric procedure developed here for the analysis of *Idiognathodus* P_1 element shape variation can be easily modified and used in the analysis of P_1 elements of other conodont taxa.

All species of the *Idiognathodus simulator* group (*I. simulator*, *I. auritus*, *I. lateralis* sp. nov., *I. luganicus*, and *I. praenuntius*) have asymmetrical P_1 element pairs. Sinistral elements are narrow, curved and elongate. Dextral elements are straight, triangular, and have a wider rostral platform area. Species of the *I. simulator* group are defined by platform shape and the presence of lobes. Some *I. simulator* group species share juvenile P_1 element morphologies and do not reach a diagnostic growth stage until the platform is longer than approximately 0.4 mm. Dextral elements of the *I. simulator* group show more allometric bias in the development of lobes and the isolation of the caudal adcarinal ridge. This suggests that sinistral elements may be better for species discrimination among smaller specimens. The concept of *I. simulator* has been restricted to asymmetrically paired P_1 elements with an eccentric groove and an isolated caudal adcarinal ridge, which should ensure consistent correlation of the Kasimovian Gzhelian boundary.

Systematic palaeontology

Illustrated specimens are reposited at the University of Iowa Paleontology Repository (SUI). All specimens included in the morphometric analyses were assigned a separate morphometric identification number (TT). Each locality has two abundance tables, one that gives the *Idiognathodus* elements as morphotype groups separated by chirality (SOM 1: tables 1, 3, and 5), and another that lists *Idiognathodus* species (SOM 1: tables 2, 4, and 6).

Class Conodonti Branson, 1938
Order Ozarkodinida Dzik, 1976
Superfamily Polygnathacea Bassler, 1925
Family Idiognathodontidae Harris and Hollingsworth, 1933
Genus *Idiognathodus* Gunnell, 1931

Type species: *Idiognathodus claviformis* Gunnell, 1931; Moscovian (Late Desmoinesian), Coal City Limestone Member, Pawnee Limestone, Marmaton Group; Lexington, Missouri, USA.

Idiognathodus simulator (Ellison, 1941) group

Remarks.—The *Idiognathodus simulator* group includes species with asymmetrical P_1 element pairs and typically with an eccentric groove running down the length of the platform. There has been some disagreement whether or not species of the *Idiognathodus simulator* group should be assigned to the genus *Streptognathodus* Stauffer and Plummer, 1932 (e.g., Chernykh 2005, 2012) or *Idiognathodus* Gunnell, 1931 (e.g., Barrick et al. 2008). We assign all these species to *Idiognathodus* for the same reasons discussed by Barrick et al. (2008). There is additional confusion about whether the P_1 elements (platforms) of the species were strongly asymmetrical, where the sinistral and dextral elements differ in morphology (class IIIb symmetry, Lane [1968]; e.g., Barrick et al. 2008), or whether the P_1 element pairs were near mirror images of each other (class II symmetry, Lane [1968]; e.g., Chernykh 2005, 2012). For these reasons, we include a complete description and diagnosis for each species of the *I. simulator* group based on the material collected from the Heebner Shale.

Species of the *Idiognathodus simulator* group are distinguished from one another primarily by the degree of development of lobes and secondarily by the shape of the platform and adcarinal ridge. Members of the *I. simulator* group are *I. auritus*, *I. lateralis* sp. nov., *I. luganicus*, *I. praenuntius*, *I. simulator*, and *I. postsimulator*. Possible synonymous species include *I. gravis*, and *I. sinistrum*, which are discussed under *I. auritus* and *I. simulator*, respectively. *Idiognathodus luosuensis* (Wang and Qi, 2003) may belong to the *I. simulator* group, but requires additional study.

The dominantly Gzhelian *Idiognathodus simulator* group is characterized by distinct asymmetry between the dextral and sinistral P_1 elements, in contrast to most other species of *Idiognathodus* in which the P_1 element pairs are approximately mirror images. A similar degree of P_1 element asymmetry, as well as an eccentric groove, can be seen in the Kasimovian species *I. eudoraensis* Barrick, Heckel, and Boardman, 2008, which was proposed to be the ancestor of *I. simulator* (Barrick et al. 2008). The beginning of the *I. eudoraensis*–*I. simulator* lineage, and the origin of the eccentric groove and P_1 element asymmetry are not known. Rosscoe (2008) reported that the somewhat older Kasimovian species *I. magnificus* Stauffer and Plummer, 1932, appears to show moderately asymmetrical variation between the dextral and sinistral P_1 elements, and it may be a possible ancestral

form. *Idiognathodus magnificus* has very large lobes ornamented with abundant nodes and lacks an eccentric groove. In many specimens, the transverse ridges appear notched, and aligned, forming a visible line down the platform, but the transverse ridges remain complete and no groove exists. Because of the likely origin from a typically ungrooved *Idiognathodus* species, *I. simulator* group species have been assigned to the genus *Idiognathodus* (Barrick et al. 2008).

Idiognathodus simulator (Ellison, 1941)

Fig. 13.

1941 *Streptognathodus simulator* sp. nov.; Ellison 1941: 133, pl. 22: 25 (holotype), 29.

1959 *Streptognathodus simulator* Ellison, 1941; Jennings 1959: 994–995, pl. 124: 7.

1972 *Streptognathodus eccentricus* Ellison, 1941; Von Bitter 1972: pl. 3: 1a, 1b, 1c?

1972 *Streptognathodus simulator* Ellison, 1941; Von Bitter 1972: 56, pl. 3: fig. 2a, 2b, 2c?, 2d.

1978 *Streptognathodus simulator* Ellison, 1941; Kozitskaya et al. 1978: 106, pl. 30: 1?, 2.

1981 *Streptognathodus eccentricus* Ellison, 1941; Barskov et al. 1981: pl. 2: 15.

1986 *Streptognathodus simulator* Ellison, 1941; Chernykh 1986: pl. 27: 22.

1987 *Streptognathodus simulator* Ellison, 1941; Barskov et al. 1987: 91, pl. 21: 14, 15.

1987 *Streptognathodus eccentricus* Ellison, 1941; Barskov et al. 1987: 87, pl. 21: 16?, 18.

1987 *Streptognathodus simulator* Ellison, 1941; Cherynkh and Reshetkova 1987: pl. 3:17–20.

1997 *Streptognathodus simulator* Ellison, 1941; Kozitskaya and Nemirovskaya 1997: pl. 10: 26?

2005 *Streptognathodus simulator* Ellison, 1941; Chernykh 2005: 138–141, pl. 1: 6; pl. 2: 1, 2, 4?, 7.

2005 *Streptognathodus sinistrum* sp. nov.; Chernykh 2005: 141, pl. 2: 8 (holotype), 9–12.

2009 *Idiognathodus simulator* (Ellison, 1941); Alekseev et al. 2009: pl. 3: 11?

2008 *Idiognathodus simulator* (Ellison, 1941); Barrick et al. 2008: 127–130, pl. 1: 4, 14, 15, 19?, 20, 21, 23.

2008 *Idiognathodus simulator* (Ellison, 1941); Heckel et al. 2008. fig. 1: 5.

2008 *Streptognathodus sinistrum* Chernykh, 2005; Davydov et al. 2008: 124, fig. 11: K, L (holotype re-illustration).

2008 *Streptognathodus simulator* Ellison, 1941; Davydov et al. 2008: 124, fig. 11: A, B?, C?, D.

2010 *Idiognathodus simulator* (Ellison, 1941); Barrick et al. 2010: pl. 9: 14.

2012 *Streptognathodus simulator* Ellison, 1941; Chernykh 2012: 81–83, pl. 6: 1, 2, 12?, 15?, 16?

2013 *Idiognathodus simulator* (Ellison, 1941); Barrick et al. 2013a: pl. 4: 9 (holotype re-illustration).

Material.—145 sinistral P_1 and 134 dextral P_1 elements. Illustrated specimens repository numbers SUI 141025–SUI 141041. Collected from the early Gzhelian Heebner Shale from all three outcrops in this study, Sedan, Clinton, and I-229 roadcut, Kansas, USA.

Diagnosis.—Asymmetrical P_1 element pair, presence of an eccentric groove, and a caudal adcarinal ridge separated from the caudal platform margin by the caudal adcarinal trough.

Description.—Sinistral P_1 element: Rostral platform margin forms a broadly curved, convex edge. Caudal platform margin is slightly curved and convex, with the point of maximum curvature located near the midpoint of the margin. Typically, the caudal platform margin does not extend to the dorsal tip of the element, and is often separated from the tip by the eccentric groove. The eccentric groove is well developed and may intersect the caudal margin before reaching the dorsal tip of the platform. Rostral adcarinal ridge is either parallel to the carina or dips in towards it. The caudal adcarinal ridge is truncated by the adcarinal trough and separated from the caudal platform margin. Generally, the ventral end of the caudal platform margin and dorsal end of the caudal adcarinal ridge overlap one another. This is a diagnostic feature of the species. In smaller specimens with a platform length less than ~0.5 mm, a tall solitary node lies outside the caudal platform and extends laterally. This juvenile state is morphologically similar to juveniles of *I. lateralis* sp. nov., but differs in having a higher node and the lateral direction of its peak. In larger specimens, the peak of the node fuses with the caudal adcarinal ridge and rises higher than the caudal platform margin, forming a parapet. The separation between the parapet and the platform margin becomes more apparent as the dorsal-ventral growth of each begins to overlap, accentuating the adcarinal trough between them. The transverse ridges on the platform typically intersect the eccentric groove at an oblique angle and are frequently aligned with one another on opposite sides of the groove. In the largest specimens a rostral lobe with one or two nodes may develop. This lobe is small in all dimensions of growth and has little effect on the curvature of the rostral platform margin and adcarinal ridge. Larger specimens typically have a wider platform relative to length than smaller specimens.

Dextral element: Rostral platform margin is widest near the ventral end and tapers inwards to the dorsal tip, giving the platform a broader, more triangular appearance than the sinistral element. Caudal platform margin is slightly convex with maximum curvature occurring near the midpoint of the margin. Rostral adcarinal ridge is short and is typically parallel to the carina, but may dip in towards it. Caudal adcarinal ridge is subparallel to the carina and its separation from the platform margin may not be obvious until the platform is approximately 0.4 mm long. This results in morphological similarity between juvenile dextral P_1 elements of *I. simulator* and *I. luganicus*. The isolated caudal adcarinal ridge appears to be more parallel to the carina in dextral elements than in sinistral elements where the ridge flares outwards. A rostral lobe on large, dextral elements is rare and less common than on sinistral elements. The eccentric groove is shifted to the caudal edge of the platform and is usually well developed. The transverse ridges on the dextral elements are subperpendicular to the eccentric groove and typically aligned with each other on opposite sides of the platform.
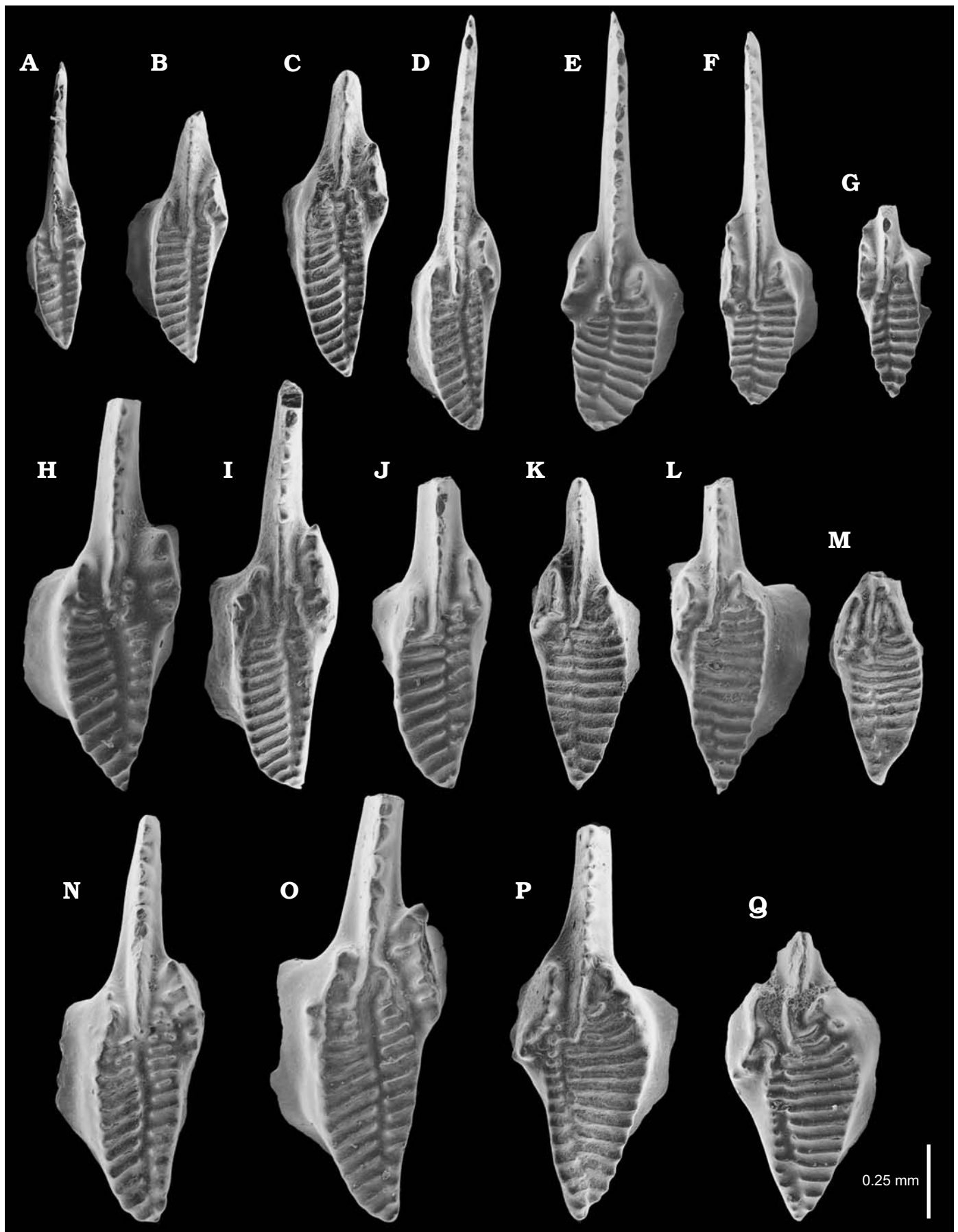
Carina typically extends dorsally to the point of the first or second ventral-most transverse ridge in most specimens.

Remarks.—The disconnected adcarinal ridge is diagnostic of *Idiognathodus simulator* and occurs on the holotype of Ellison (1941). Chernykh (2005) diagnosed *S. sinistrum* Chernykh, 2005, as having a high, isolated, parapet. Specimens of *I. sinistrum* illustrated by Chernykh (2005) and Davydov et al. (2008) appear to be small sinistral specimens of *I. simulator.* Illustrations of *I. simulator* in Davydov et al. (2008) are larger specimens that have a rostral lobe. Most of these specimens (Davydov et al. 2008: fig. 11A–D) appear to have the diagnostic isolated and outward flaring adcarinal ridge of *I. simulator*, and also have a broader platform than the illustrated specimens of *S. sinistrum.* Widening of the platform and development of a rostral lobe are characteristics that develop during growth in *I. simulator* and are typically only seen in larger specimens. Davydov et al. (2008) also record that *I. simulator* and *S. sinistrum* have the same stratigraphic occurrence. We interpret *S. sinistrum* to be a junior synonym of *I. simulator.* Davydov et al. (2008) stated that North American specimens have a more elongate and asymmetrical platform than specimens from the Urals, which are more isometric in platform shape. Both elongate forms (Fig. 13B–D, K, L) and more isometric forms (Fig. 13E, F, H–J, Q) with the diagnostic adcarinal ridge are present in the Heebner Shale.

The specimen illustrated as *Streptognathodus simulator* by Jennings (1959: pl. 124: 7) appears to have a slight separation between the adcarinal ridge and the platform margin, and we consider it to belong to *Idiognathodus simulator,* even though the separation is faint. In the specimen illustrated as *I. tersus* by Zagorodnyuk et al. (1979: pl. 35: 7) the caudal adcarinal ridge appears to be separated from the platform margin, but it difficult to tell from the illustration. Specimens illustrated as *I. simulator* by Chernykh (1986: pl. 27: 20, 21) belong to the *I. simulator* group. However, the photo quality makes it difficult to be certain whether these specimens belong to *I. simulator* or *I. lateralis* sp. nov.

Stratigraphic and geographic range.—Early Gzhelian, *Idiognathodus simulator* Zone. Midcontinent North America, Donets Basin, southern, western, and central Urals, Moscow Basin, south China.

Idiognathodus auritus (Chernykh, 2005)

Fig. 14.

1959 *Streptognathodus eccentricus* Ellison, 1941; Jennings 1959: 995, pl. 124: 9.
1972 *Streptognathodus eccentricus* Ellison, 1941; Von Bitter 1972: pl. 3: 1d.
1975 *Streptognathodus simulator* Ellison, 1941; Barksov and Alekseev 1975: pl. 2: 19.

1978 *Streptognathodus eccentricus* Ellison, 1941; Kozitskaya et al. 1978: 91–92, pl. 30: 6–7.
1983 *Streptognathodus eccentricus* Ellison, 1941; Kozitskaya 1983: pl. 1: 27, 28.
1983 *Streptognathodus simulator* Ellison, 1941; Kozitskaya 1983: pl. 1: 33?
1984 *Streptognathodus eccentricus* Ellison, 1941; Alekseev et al. 1984: pl. 1: 12, 14, 18?
1984 *Streptognathodus simulator* Ellison, 1941; Alekseev et al. 1984: pl. 1: 20, 21.
1986 *Streptognathodus simulator* Ellison, 1941; Alekseev et al. 1986: 134, pl. 34: 9, 12.
1987 *Streptognathodus eccentricus* Ellison, 1941; Barskov et al. 1987: 87, pl. 21: 17, 19.
2005 *Streptognathodus auritus* sp. nov.; Chernykh 2005: 125, pl. 3: 2 (holotype), 3, 6, 7.
2005 *Streptognathodus* aff. *auritus*; Chernykh 2005: pl. 3: 1.
2005 *Streptognathodus simulator* Ellison, 1941; Chernykh 2005: 138–141, pl. 2: 2?, 4?
2005 *Streptognathodus* aff. *simulator*; Chernykh 2005: pl. 2: 5.
2008 *Streptognathodus auritus* Chernykh, 2005; Davydov et al. 2008: 130, fig. 11F?, G (holotype re-illustration).
2008 *Streptognathodus simulator* Ellison, 1941; Davydov et al. 2008: 124, fig. 11B?, C?
2009 *Idiognathodus* ex gr. *simulator*; Alekseev et al. 2009: pl. 5: 2, 3, 7, 8, 10, 12, 13; pl. 3: 1?, 2, 4–6, 7?, 9, 10?, 13, 14?
2009 *Idiognathodus simulator* (Ellison, 1941); Alekseev et al. 2009: pl. 5: 7, pl. 3: 8, 11.
2009 *Idiognathodus sinistrum* (Chernykh, 2005); Alekseev et al. 2009: pl. 5: 4.
2010 *Idiognathodus simulator* (Ellison, 1941); Barrick et al. 2010: pl. 9: 5, 11–13.
2010 *Idiognathodus simulator* (Ellison, 1941); Goreva and Alekseev 2010: pl. 1: 11, 12?
2012 *Streptognathodus simulator* Ellison, 1941; Chernykh 2012: 81–83, pl. 6: 3–7, 8?, 11, 12?, 13, 14, 15?, 17, 18, 20, 21.
2012 *Streptognathodus* aff. *auritus*; Chernykh 2012: 81–83, pl. 6: 17, 18, 20.

Material.—156 sinistral P_1 and 29 dextral P_1. Illustrated specimens repository numbers SUI 141042–SUI 141054. Collected from the early Gzhelian Heebner Shale from all three outcrops in this study, Sedan, Clinton, and I-229 roadcut, Kansas, USA.

Diagnosis.—Asymmetrical P_1 element pair, presence of an eccentric groove. Sinistral elements with flared adcarinal ridges and caudal and rostral lobes. Dextral elements with a flared rostral adcarinal ridge and a caudal lobe.

Description.—Sinistral element: Rostral platform margin is broadly curved, with the maximum curvature located near the midpoint or on the ventral half of the margin. Caudal platform margin is curved along its entire length with its maximum curvature near the midpoint or just dorsal of the midpoint the margin. Both adcarinal ridges flare ventrally away from the carina and are concave along their entire

← Fig. 13. Conodont P_1 elements of *Idiognathodus simulator* (Ellison, 1941) from the Heebner Shale, Gzhelian (Late Pennsylvanian). **A**. SUI 141025 (TT0312); Sedan 19. **B**. SUI141026 (TT0248); Clinton 14. **C**. SUI 141027 (TT0244); Clinton 12. **D**. SUI 141028 (TT0252); Sedan 11. **E**. SUI 141029 (TT0149); Sedan 20. **F**. SUI 141030 (TT0103); Sedan 15. **G**. SUI 141031 (TT0313); Sedan 16. **H**. SUI 141032 (TT0192); Sedan 16. **I**. SUI 141033 (TT0247); Clinton 13. **J**. SUI 141034 (TT0077); I229-82. **K**. SUI 141035 (TT0292); Clinton 12. **L**. SUI 141036 (TT0157); Clinton 20. **M**. SUI 141037 (TT0291); Clinton 12. **N**. SUI 141038 (TT0193); Sedan 16. **O**. SUI 141039 (TT0076); I229-82. **P**. SUI 141040 (TT0290); Clinton 12. **Q**. SUI 141041 (TT0158); I229-92.
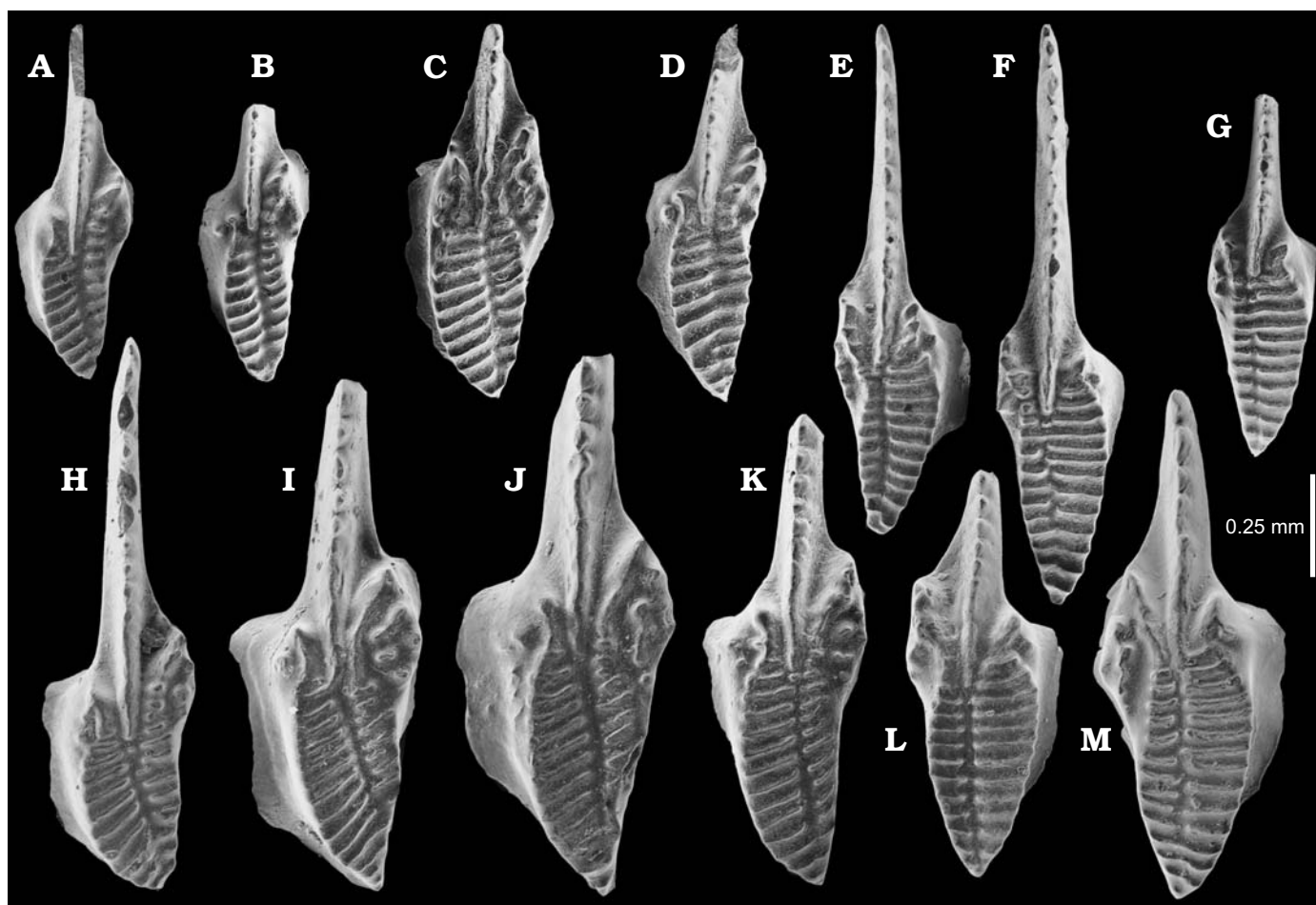
Fig. 14. Conodont P₁ elements of *Idiognathodus auritus* (Chernykh, 2005) from the Heebner Shale, Gzhelian (Late Pennsylvanian). **A**. SUI 141042 (TT0314); Sedan 17. **B**. SUI 141043 (TT0311); Sedan 24. **C**. SUI 141044 (TT0251); Sedan 11. **D**. SUI 141045 (TT0222); Clinton 12. **E**. SUI 141046 (TT0251); Sedan 11. **F**. SUI 141047 (TT0235); Sedan 11. **G**. SUI 141048 (TT0256); Sedan 11. **H**. SUI 141049 (TT0095); I229-83. **I**. SUI 141050 (TT0093); Clinton 21. **J**. SUI 141051 (TT0094); I229-83. **K**. SUI 141052 (TT0221); Clinton 12. **L**. SUI 141053 (TT0169); Sedan 23. **M**. SUI 141054 (TT0167); Sedan 23.

length. The concavity formed by the adcarinal ridges and the ventral portion of both platform margins forms a rostrum, with lobes occurring outside the concavity. The lobe and margin concavity extend farther dorsally along the caudal side than along the rostral side. The caudal lobe typically bears one to four nodes, with the number of nodes increasing as the specimen increases in size. The rostral lobe is smaller and usually bears just one or two nodes. The carina is straight and terminates at the point of maximum concavity of the rostrum. The eccentric groove is typically well developed and often terminates along the caudal margin just before reaching the dorsal tip. The groove is shifted to the caudal side resulting in the rostral platform comprising roughly two-thirds of the overall platform area. Transverse ridges intersect the groove at an oblique angle, and are usually aligned with each another on opposite sides of the groove. Development of the rostral lobe occurs slightly later in growth than the caudal lobe, but both can consistently be seen at a platform length of approximately 0.5 mm.

Dextral element: Rostral platform margin is broadly curved and the maximum curvature is located along the ventral half of the margin. Caudal platform margin is curved, with maximum curvature near the midpoint or along the dorsal half of the margin. Both caudal and rostral adcarinal ridges flare away from the carina and the caudal ridge is the longer of the two. The caudal lobe usually bears one to three nodes, with the number of nodes increasing with size. A rostral lobe is rare and only occurs in larger specimens. When a rostral lobe is present, it is small, with just one node. The rostral adcarinal ridge flares ventrally outwards even in the absence of a rostral lobe. Transverse ridges are sub-perpendicular to the eccentric groove and are aligned with each other on opposite sides of the groove. Groove development is variable in dextral elements, but is often complete, and caudally shifted such that the rostral platform area composes approximately two-thirds of the total platform area. The carina terminates at the location of maximum curvature of the rostrum formed by the two adcarinal ridges.

Remarks.—The flaring adcarinal ridges and the rostral lobe are the primary diagnostic characters of *Idiognathodus auritus* and the species includes sinistral and dextral elements with both caudal and rostral lobes, and dextral elements

with only a caudal lobe and a flared rostral adcarinal ridge. The asymmetry in P_1 elements is more than just overall shape variation, but includes the development of a lobe on the rostral side. Both sinistral and dextral elements have a caudal lobe at sizes exceeding a platform length of 0.4 mm. However, the rostral lobe is commonly seen on sinistral elements and rarely on dextral elements. Dextral elements with a rostral lobe are typically large, but have the diagnostic flared rostral adcarinal ridge as seen in smaller specimens. Because two-lobed sinistral elements were more common relative to dextral elements and the co-occurrence of two-lobed sinistral elements with one-lobed dextral elements that have flared adcarinal ridges, it is inferred that some two-lobed sinistral elements were paired with one-lobed dextral elements. In this study, dextral specimens without a rostral lobe that could not be confidently classified as *I. auritus* based on their shape were classified as *I. lateralis* sp. nov. based on their lobe character state.

Chernykh (2012) described the two-lobed species *Streptognathodus gravis,* which appears to differ from *I. auritus* because it does not show rostral ridge flaring, has a larger rostral lobe, and because the platform tends to taper dorsally without as much curvature along the platform margins.

Stratigraphic and geographic range.—Early Gzhelian, *Idiognathodus simulator* Zone. Midcontinent North America, Donets Basin, southern and western Urals, Moscow Basin, south China.

Idiognathodus lateralis sp. nov.
Fig. 15A–M.

1941 *Streptognathodus simulator* sp. nov.; Ellison 1941: 133, pl. 22: 27, 28, 30 (only).
1978 *Streptognathodus simulator* Ellison, 1941; Kozitskaya et al. 1978: 106, pl. 30: 3.
1983 *Streptognathodus simulator* Ellison, 1941; Kozitskaya 1983: pl. 1: 30.
1987 *Streptognathodus simulator* Ellison, 1941; Cherynkh and Reshetkova 1987: pl. 2: 19, 20.
1996 *Streptognathodus eccentricus* Ellison, 1941; Sobolev and Nakrem 1996: 73–74, pl. 5: B.
2003 *Idiognathodus simulator* Ellison, 1941; Wang and Qi 2003: pl. 4: 9.
2005 *Streptognathodus luganicus* Kozitskaya, 1978; Chernykh 2005: pl. 3: 8.
2005 *Streptognathodus simulator* Ellison, 1941; Chernykh 2005: 138–141, pl. 2: 3.
2006 *Streptognathodus simulator* Ellison, 1941; Boardman et al. 2006: pl. 1: 9, 10.
2008 *Idiognathodus simulator* (Ellison, 1941); Barrick et al. 2008: 127–130, pl. 1: 3?, 9?, 10–12, 18, 22.
2008 *Idiognathodus simulator* (Ellison, 1941); Heckel et al. 2008: fig. 1: 6.
2009 *Idiognathodus ex gr. simulator*; Alekseev et al. 2009: pl. 5: 6.
2010 *Idiognathodus simulator* (Ellison, 1941); Barrick et al. 2010: pl. 9: 7–9.
2012 *Streptognathodus simulator* Ellison, 1941; Chernykh 2012: 81–83, pl. 6: 8?, 10, 19.
2013 *Idiognathodus simulator* (Ellison, 1941); Barrick et al. 2013a: pl. 4: 10.
2013 *Idiognathodus simulator* (Ellison, 1941); Barrick et al. 2013b: fig. 10: 9.

Etymology: From Latin *lateralis*, side; referring to the side or flank.
Holotype: Sinistral P_1 element SUI 141070; TT00039 (Fig. 15I).
Type horizon: Early Gzhelian, Late Pennsylvanian.
Type locality: Heebner Shale Member of the Oread Formation, sample 19, Clinton section, Kansas, USA.

Material.—891 sinistral P_1 and 756 dextral P_1 elements. Illustrated specimens repository numbers SUI 141062–SUI 1410474. Collected from the early Gzhelian Heebner Shale from all three outcrops in this study, Sedan, Clinton, and I-229 roadcut, Kansas, USA.

Diagnosis.—Asymmetrical P_1 element pair, one lobe on the caudal side, a caudally shifted eccentric groove, the platform margins and adcarinal ridges form continuous boundaries, and the caudal lobe is located outside of the adcarinal ridge.

Description.—*Sinistral element*: Rostral platform is broadly curved with the point of maximum curvature located near the midpoint of the margin. Rostral adcarinal ridge is either parallel to the carina or follows the curvature of the platform margin, forming a continuous curve from the dorsal tip to the end of the adcarinal ridge. Caudal platform margin can be straight and tapered, or show minor curvature, with the maximum curvature occurring along the dorsal half of the margin. Caudal adcarinal ridge flares away from the carina and is typically concave near the lobe. Specimens with a straighter caudal platform margin show less adcarinal ridge concavity near the lobe than the specimens that are more curved along the platform margin. Carina terminates dorsally near the most ventral transverse ridges. Eccentric groove is usually well developed and is shifted to the caudal margin of the platform. The eccentric groove is shifted closer to the caudal margin in specimens that have a straighter caudal platform margin, and the caudal platform area may represent only about ¼ of the total platform area. Oral platform surface typically dips inwards towards the eccentric groove on both sides of the groove. The eccentric groove either extends to the dorsal tip or terminates on the caudal margin of the element near the dorsal tip. Transverse ridges intersect the eccentric groove at an oblique angle and vary in alignment to each other on opposite sides of the groove. The caudal lobe appears in small specimens with a platform length of 0.3–0.4 mm. The lobe has one node until the platform reaches a length of approximately 0.5 mm. At this size a second or third node may develop, but these are often smaller in size than the original node. The lobe often terminates near the first or second transverse ridge, dorsally to the adcarinal ridge.

Dextral element: Rostral platform margin is widest near the ventral end and tapers straight to the dorsal tip, producing a wide ventral platform region. Caudal platform margin is slightly curved, concave near the lobe, and is usually most curved from near the midpoint to the dorsal half of the margin. In some specimens the caudal platform can be nearly straight and smaller specimens tend to have straighter caudal margins than larger specimens. As the element increase
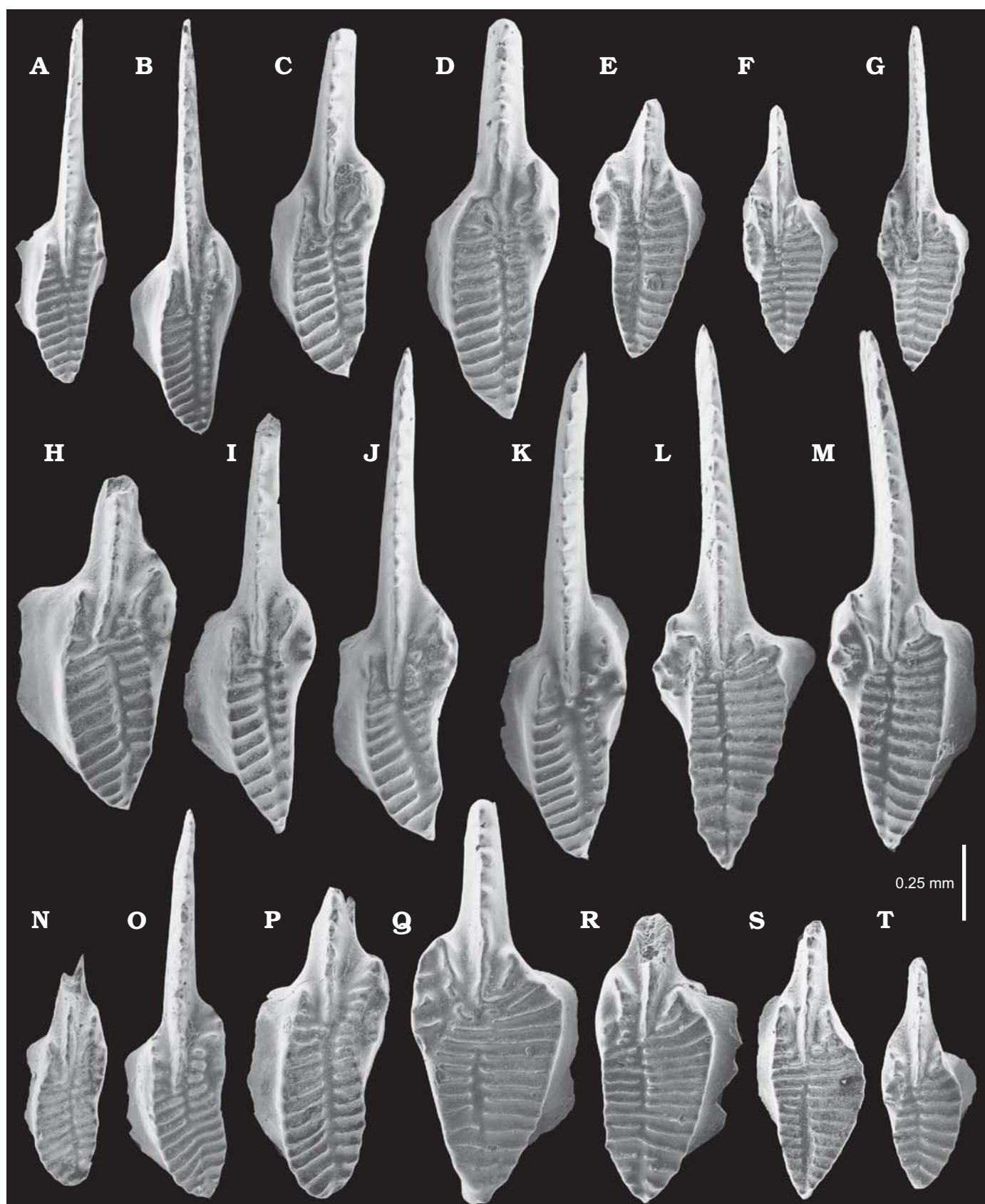
Fig. 15. Conodont P$_1$ elements of *Idiognathodus lateralis* sp. nov. (**A–M**) and *Idiognathodus praenuntius* (Chernykh, 2005) (**N–T**) from the Heebner Shale, Gzhelian (Late Pennsylvanian). **A**. SUI 141062 (TT0228); Sedan 11. **B**. SUI 141063 (TT0233); Sedan 11. **C**. SUI 141064 (TT0050); Clinton 20. **D**., SUI 141065 (TT0019); Clinton 22. **E**. SUI 141066 (TT0168); Sedan 23. **F**. SUI 141067 (TT0261); Sedan 11. **G**. SUI 141068 (TT0260); Sedan 11. →

in size, both ventral platform margins increase greatly in width and become straighter, giving the platform a triangular shape. Rostral adcarinal ridge is very short and may appear as a small node above the most ventral transverse ridge. The rostral adcarinal ridge is either parallel to the carina or dips in towards it. The caudal adcarinal ridge is much longer, and flares away from the carina. The eccentric groove is more weakly developed in dextral elements than in sinistral elements, and can vary in its depth and width along the entire length of the groove. Transverse ridges are sub-perpendicular to the eccentric groove and are typically aligned with each other on opposite sides of the groove. Platform surface is generally flat, but may dip in towards the eccentric groove. The caudal lobe can extend dorsally to the midpoint of the platform margin. Often, the junction of the dorsal termination of the lobe and the platform margin is, or is near to, the point of maximum curvature along the platform margin. The concavity along the platform margin and the adcarinal ridge associated with the lobe is typically broad and smooth.

Remarks.—*Idiognathodus lateralis* sp. nov. is the most abundant species collected from the Heebner Shale. The asymmetric P_1 element pair, single caudal lobe, strongly caudally shifted eccentric groove, the continuous boundary formed by the caudal margin and the caudal adcarinal ridge, and asymmetrical platform margins are the diagnostic features of this species. The restriction of *I. simulator* to P_1 elements with an isolated caudal adcarinal ridge leaves many specimens previously assigned to *I. simulator* without a species designation, most of which are placed within *I. lateralis* sp. nov. *Idiognathodus lateralis* sp. nov. is similar to *I. praenuntius* (Chernykh, 2005) and the two are distinguished by the location of the eccentric groove and the shape of the platform margins. In *I. lateralis* sp. nov. the eccentric groove is shifted more strongly caudally and the platform margins are more asymmetrical than in *I. praenuntius*. There is some degree of subjectivity in distinguishing a more medial groove from a caudally shifted one. However, specimens with a more medial groove frequently have more symmetrical platform margins, with curvature occurring at the same length along each margin. Juvenile sinistral elements and dextral elements of *I. auritus* (Chernykh, 2005) that only have a caudal lobe can be distinguished from *I. lateralis* by the outwards flaring of the rostral adcarinal ridge, which can be seen before a rostral lobe is developed.

Asymmetry between the sinistral and dextral P_1 elements of *Idiognathodus lateralis* sp. nov. increases as the size of the specimens increases, with the sinistral elements being more similar to the smaller elements, and the dextral elements becoming very different in shape at larger sizes. Dextral elements appear to grow to a maximum platform length of approximately 0.75 mm and then expand laterally, forming

broad, and flat oral platform surfaces, and triangular platform shapes. Sinistral elements typically have an oral platform surface that dips inwards towards the eccentric groove, and maintain their relative platform length and width dimensions at all growth stages. In large specimens the eccentric groove is typically better developed on the sinistral element than the dextral element. The lobe of the dextral element is more dorsally-ventrally expansive and larger than the lobe on the sinistral element, except for in larger specimens, where the lobe may become wider. Nodes on the dextral element lobe have a greater tendency to be more numerous, fused, or elongated in shape, and sometimes appear as parapets. Sinistral element lobe nodes are typically domal in shape, and the lobe is not as large as the lobe on the dextral element.

Stratigraphic and geographic range.—Early Gzhelian, *Idiognathodus simulator* Zone. Midcontinent North America, south-central New Mexico, Donets Basin, southern and central Urals, Novaya Zemlya, Arctic Russia, Moscow Basin, south China.

Idiognathodus luganicus (Kozitskaya, 1978)

Fig. 16.

1978 *Streptognathodus luganicus* sp. nov.; Kozitskaya et al. 1978: 101–102, pl. 30: 10 (holotype), 11.

1979 *Streptognathodus simulator* Ellison, 1941; Zagorodnyuk et al. 1979: pl. 36: 13.

1987 *Streptognathodus luganicus* Kozitskaya, 1978; Cherynkh and Reshetkova 1987: pl. 3: 16.

1995 *Streptognathodus simulator* Ellison, 1941; Henderson et al. 1995: pl. 1: 9.

1996 *Streptognathodus luganicus* Kozitskaya, 1978; Sobolev and Nakrem 1996: 79, pl. 5: A?

1997 *Streptognathodus luganicus* Kozitskaya, 1978; Kozitskaya and Nemirovskaya 1997: pl. 10: 25.

2006 *Streptognathodus luganicus* Kozitskaya, 1978; Boardman et al. 2006: pl. 1: 7.

2006 *Streptognathodus simulator* Ellison, 1941; Boardman et al. 2006: pl. 1: 8.

2009 *Idiognathodus luganicus* (Kozitskaya, 1978); Alekseev et al. 2009: pl. 5: 5.

2009 *Idiognathodus ex gr. simulator*; Alekseev et al. 2009: pl. 5: 9.

2009 *Idiognathodus simulator* (Ellison, 1941); Alekseev et al. 2009: pl. 5: 11.

2007 *Idiognathodus lobulatus* Kozitskaya, 1978; Sudar et al. 2007: pl. 2: 6?

2008 *Idiognathodus simulator* (Ellison, 1941); Barrick et al. 2008: 127–130, pl. 1: 5, 13, 16, 17.

2008 *Streptognathodus simulator* Ellison, 1941; Davydov et al. 2008: 124, fig. 11E.

Material.—403 sinistral P_1 and 516 dextral P_1 elements. Illustrated specimens repository numbers SUI 141094 –SUI 141104. Collected from the early Gzhelian Heebner Shale from all three outcrops in this study, Sedan, Clinton, and I-229 roadcut, Kansas, USA.

H. SUI 141069 (TT0064); Clinton 29. **I**. Holotype, SUI 141070 (TT0039); Clinton 19. **J**. SUI 141071 (TT0049); Clinton 28. **K**. SUI 141072 (TT0034); Sedan 20. **L**. SUI 141073 (TT0185); Clinton 37. **M**. SUI 141074 (TT0170); Sedan 20. **N**. SUI 141075 (TT0214); Clinton 18. **O**. SUI 141076 (TT0066); Clinton 27. **P**. SUI 141077 (TT0055); Sedan 23. **Q**. SUI 141078 (TT0176); Clinton 19. **R**. SUI 141079 (TT0188); Clinton 29. **S**. SUI 141080 (TT0269); Sedan 11. **T**. SUI 141081 (TT0264); Sedan 11.
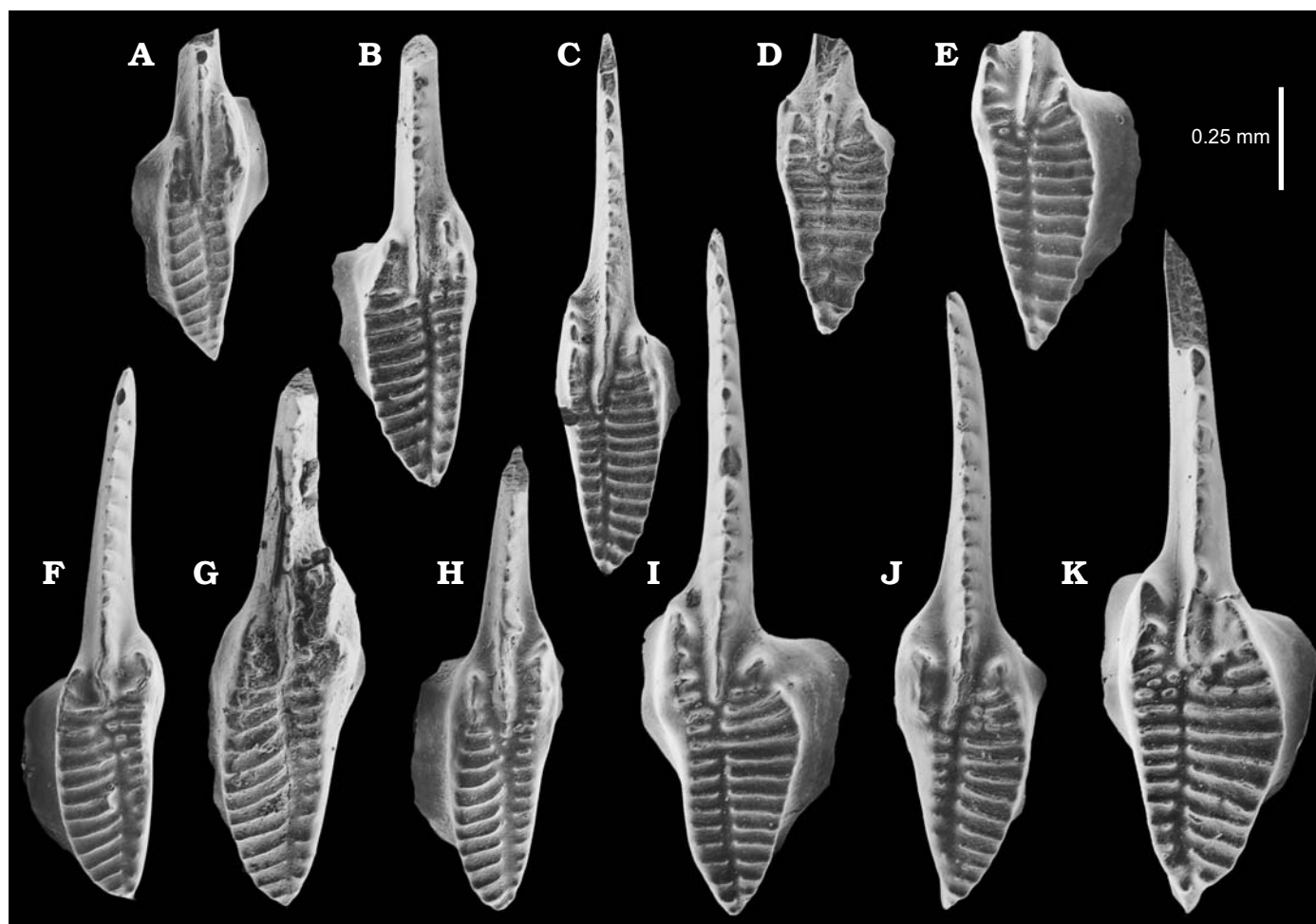
Fig. 16. Conodont P₁ elements of *Idiognathodus luganicus* (Kozitskaya, 1978) from the Heebner Shale (Gzhelian, Late Pennsylvanian). **A**. SUI 141094 (TT0200); Sedan 11. **B**. SUI 141095 (TT0209); Clinton 12. **C**. SUI 141098 (TT0285); Clinton 12. **D**. SUI 141096 (TT0284); Clinton 12. **E**. SUI 141097 (TT0141); Clinton 28. **F**. SUI 141099 (TT0018); Clinton 15. **G**. SUI 141100 (TT0026); I229-83. **H**. SUI14101 (TT0016); Clinton 14. **I**. SUI 14102 (TT0119); Sedan 20. **J**. SUI 141103 (TT0118); Sedan 20. **K**. SUI 141104 (TT0102); Sedan 12.

Diagnosis.—Asymmetrical P₁ element pair, presence of an eccentric groove, and absence of lobes on caudal and rostral platform margins.

Description.—Sinistral P₁ element: Rostral platform margin is slightly curved along the dorsal half and typically straight along the ventral half. Caudal platform margin is relatively straight and the point of maximum curvature is located on the dorsal half of the margin. The caudal adcarinal ridge is longer than the rostral ridge and extends parallel to the carina. The rostral adcarinal ridge is reduced in length and may appear as a small node extending from the rostral platform margin. The rostral adcarinal ridge is typically parallel to the carina or dips towards it at an angle less than 45°. The carina ends ventrally of the transverse ridges, and is relatively longer in smaller specimens. The eccentric groove is frequently deeper on sinistral elements than dextral elements and is shifted caudally, such that the caudal platform area comprises approximately 1/3 of the total platform area. The groove is developed at all ontogenetic stages, but is occasionally constricted by transverse ridge growth. Platform surface appears in two styles. In one, a flat oral surface with little relief to the eccentric groove occurs. In the other, the oral surface slants inwards towards the eccentric groove. The latter platform is more abundant in smaller elements and in elements with an eccentric groove that is strongly shifted caudally. The platform grows predominately lengthwise until it is approximately 0.5 mm in length. At that point the platform starts to widen and the eccentric groove becomes more weakly developed. Transverse ridges tend to be slightly oblique to the eccentric groove on both sides of the platform. In some cases the transverse ridges on opposite sides of the groove are nearly aligned and in other cases they may dip dorsally from one another at the groove.

Dextral P₁ element: Rostral platform margin is not a long, smooth curve like it is on sinistral elements, but is wider in the ventral region. In larger forms the ventral margin forms a "shoulder" that tapers straight to the dorsal tip. This lateral growth is less apparent in smaller specimens. The caudal platform margin is relatively straight and parallel to the carina. In many larger specimens a geniculation point is located at the junction of the plat-

form margin and the adcarinal ridge. This results in the adcarinal trough being shifted outwardly, but it still lies sub-parallel to the adcarinal ridge and the caudal platform margin. Specimens lacking the elongate and laterally shifted adcarinal ridge have an adcarinal ridge that is in line with the platform margin, still longer than the rostral adcarinal ridge, but relatively short. The carina terminates ventrally of the transverse ridges except for occasional rostral transverse ridges. The eccentric groove is shallower than the groove in the sinistral elements and is shifted caudally, resulting in a rostral platform area that makes up approximately ⅔ of the total platform. The platform surface tends to be relatively flat across the oral surface, but can occasionally slant inwards towards the eccentric groove. The transverse ridges are sub-perpendicular to the eccentric groove and are often aligned with each another on opposite sides of the groove.

Remarks.—The outward shifting of the caudal adcarinal ridge in the dextral element of *Idiognathodus luganicus* creates a caudal margin similar to that in dextral elements of *I. simulator*. However, the adcarinal trough of *I. simulator* separates the adcarinal ridge from the platform margin, whereas they are not separated in *I. luganicus*. *Idiognathodus luganicus* and *I. simulator* appear to have a similar juvenile dextral element. Only at a platform length of approximately 0.4 mm does the adcarinal ridge begin to clearly disconnect from the platform margin in *I. simulator*. Specimens of *I. luganicus* exhibit one of two platform morphologies. The first has a broader, more asymmetrical platform that is similar to *I. simulator*. The second is typically a straight, more elongate, and narrower element with a lesser degree of asymmetry than the broader morphology. The holotype of *I. luganicus* is a dextral element with the more asymmetrical P₁ element pair.

Chernykh (2012) described another grooved, lobeless species, *Streptognathodus postsimulator* Chernykh, 2012, which differs from *Idiognathodus luganicus* on the basis of platform shape. Sinistral and dextral elements of *S. postsimulator* show the same pattern of asymmetry as *I. luganicus*, with a broader dextral element and a more slender sinistral element. The sinistral elements of *S. postsimulator* differ from *I. luganicus* by having an oblique eccentric groove that is aligned with the carina, a more tapered element along both platform margins, a dorsal tip that is shifted caudally out of alignment with the carina, and shorter adcarinal ridges, with the caudal ridge extending further ventrally than the rostral one. Dextral forms of *S. postsimulator* are also heavily tapered along both margins, but differ from the sinistral forms in the location of maximum curvature along the caudal platform margin.

Some specimens illustrated as *Idiognathodus simulator* by Barrick et al. (2010: pl. 9: 6, 10) should be classified as *I. luganicus* under the taxonomic scheme used here. However, these specimens are atypical from specimens observed from the Heebner Shale and possess a flaring rostral adcarinal ridge. Another atypical specimen illustrated as *Streptognathodus luganicus* by Sobolev and Nakrem (1996:

pl. 5: A) has relatively long adcarinal ridges, with the rostral adcarinal ridge being much longer than the caudal ridge.

Stratigraphic and geographic range.—Early Gzhelian *Idiognathodus simulator* Zone. Midcontinent North America, Ellesmere Island Arctic Canada, Donets Basin, Novaya Zemlya Arctic Russia, southern Urals, central Urals, Moscow Basin, Serbia.

Idiognathodus praenuntius (Chernykh, 2005)

Fig. 15N–T.

1983 *Streptognathodus simulator* Ellison, 1941; Kozitskaya 1983: pl. 1: 31, 32.
1987 *Idiognathodus* aff. *lobulatus*; Cherynkh and Reshetkova 1987: pl. 1: 11, 12.
2005 *Streptognathodus praenuntius* sp. nov.; Chernykh 2005: 135–136, pl. 1: 1–4, 5 (holotype).
2008 *Streptognathodus praenuntius* Chernykh, 2005; Davydov et al. 2008: 126–128, fig. 10: M (holotype re-illustration), N, O.
2009 *Idiognathodus* ex gr. *simulator*; Alekseev et al. 2009: pl. 3: 3.
2012 *Streptognathodus praenuntius* Chernykh, 2005; Chernykh 2012: 79–80, pl. 2: 5–9.

Material.—60 sinistral P₁ and 17 dextral P₁ elements. Illustrated specimens repository numbers SUI 141075–141081. Collected from the early Gzhelian Heebner Shale from all three outcrops in this study, Sedan, Clinton, and I-229 roadcut, Kansas, USA.

Diagnosis.—Asymmetrical P₁ element pair, presence of a slightly eccentric often interrupted groove, a caudal lobe, and nearly symmetrical platform margins.

Description.—*Sinistral element*: Rostral and caudal platform margins are broadly curved and the maximum curvature on each lies at nearly the same location on the margin, generally near the midpoint. The oral platform surface dips in towards the eccentric groove, which is complete in most specimens. The eccentric groove is shifted only slightly towards the caudal side. The transverse ridges either intersect the groove at a nearly perpendicular orientation, or they radiate from the center of the platform, changing their orientation along the length of the platform. The rostral adcarinal ridge is short and is either subparallel to the carina or flares inwards towards the carina. The caudal adcarinal ridge is longer than the rostral ridge and flares away from the carina. The caudal adcarinal ridge and platform margin are concave near the caudal lobe. The caudal lobe does not extend far along the length of the platform. The lobe is ornamented with one or two nodes. The carina terminates either ventrally of the transverse ridges, or extends into the platform to the first few ventral transverse ridges.

Dextral element: The platform is relatively short and squat. Rostral platform margin is curved with the point of maximum curvature located along the ventral portion and tapers in a slightly straighter direction to the dorsal tip. Caudal platform margin is curved and reaches maximum curvature near the midpoint of the margin. The rostral adcarinal ridge is typically parallel to the carina or dips slightly inward towards it. The caudal adcarinal ridge can

also be subparallel to the carina or dip slightly away from it. The eccentric groove is shifted slightly caudally. A lobe occurs only on the caudal side and on larger elements the number of nodes increases, often resulting in large specimens with chaotic node architecture. Transverse ridges tend to dip at a slightly oblique angle towards the eccentric groove, but are usually more parallel in the ventral half of the platform. Oral platform surface is generally flat, but may dip slightly inward toward the eccentric groove. This dip is far less pronounced in the dextral element than the sinistral element. The eccentric groove is typically thin and is typically truncated by complete transverse ridges. In larger specimens the most ventral rostral transverse ridges flare ventrally.

Remarks.—*Idiognathodus praenuntius* is the least common of the species of the *I. simulator* group recovered from the Heebner Shale. Assignment of specimens to *I. praenuntius* was based on the combination of platform margin symmetry and a more medially located groove. Also, *I. praenuntius* has an oral platform surface that dips inwards towards the middle of the element, forming a diagnostic bowl-shape. Chernykh (2005, 2012) described *I. praenuntius* as having a rhombic platform and a nearly medial groove, and his illustrated specimens are dextral elements with one caudal lobe. Davydov et al. (2008) stated that the more medial and less developed groove were diagnostic of *I. praenuntius*, but added that the near medial position of the groove is variable. In our collections, sinistral elements typically have a better developed groove than the dextral elements. Platform margin symmetry also tends to increase with a more medially positioned groove. In addition to the features listed above, the platform of *I. praenuntius* is shorter, more squat, and more ovate than the platforms of *I. auritus*, *I. simulator*, *I. lateralis* sp. nov., and *I. luganicus*.

Small dextral elements of *Idiognathodus praenuntius* and *I. lateralis* sp. nov. are similar and difficult to distinguish. Questionable specimens were assigned to *I. lateralis* sp. nov. In some samples, numerous sinistral specimens of *I. praenuntius* could be identified, but no truly diagnostic dextral elements. Dextral forms are more diagnostic at larger growth stages, as is shown by the specimens illustrated by Chernykh (2005, 2012). Distinctive larger dextral elements of *I. praenuntius* are squatter and shorter than dextral elements of *I. lateralis* sp. nov.

Specimens illustrated as *Idiognathodus praenuntius* by Barrick et al. (2010: pl. 7: 9–24) from south China appear to have a more medial groove than *I. lateralis* sp. nov. and *I. simulator*. However, the platform shape is more elongate and tapered than any specimens of *I. praenuntius* described by Chernykh (2005, 2012), or recovered in this study. The rostral ridges of the dextral elements also appear to be more elongate than typical *I. praenuntius*.

Stratigraphic and geographic range.—Early Gzhelian *Idiognathodus simulator* Zone. Midcontinent North America, Donets Basin, southern and central Urals, Moscow Basin.

Acknowledgments

References

Adams, D.C., Rholf, F.J., and Slice, D.E. 2004. Geometric morphometrics: ten years of progress following the 'revolution'. *Italian Journal of Zoology* 71: 5–16.

Alekseev, A.S., Barskov, I.S., and Migdisova, A.V. 1984. On conodonts from the Gzhelian/Kasimovian (Upper Carboniferous) boundary beds in the Rusavinko quarry (Moscow District) [in Russian]. *In*: V.V. Menner (ed.), *Paleontologičeskaâ harkteristika stratotipičeskih i oponyh razrezov Karbona Moskovskoj sineklizy (konodonty, cefalopody)*, 15–34. Izdatel'stvo Moskovskogo Universiteta, Moskva.

Alekseev, A.S., Barskov, I.S., Khalymbadzha, V.G. [Khalymbadža, V.G.], Gaptulkadyrov, M.M., and Isakova, T.N. 1986. Order Conodontophorida [in Russian]. *In*: A.D. Grigorieva and I.S. Muraviev (eds.), *Atlas fauny verhnego Karbona i nižnej Permi Samarskoj luki*, 128–135. Kazan University Press, Kazan.

Alekseev, A.S., Goreva, N.V., Isakova, T.N., Kossovaya, O.L. Lazarev, S.S., and Davydov, A.E. 2009. Gzhel section. Stratotype of the Gzhelian Stage. *In:* A.S. Alekseev and N.N. Goreva (eds.), *Type and Reference Carboniferous Sections in the South Part of the Moscow Basin. Field Trip Guidebook of the I.U.G.S. Subcommission on Carboniferous Stratigraphy*, 115–137. Borissiak Paleontological Institute of Russian Academy of Science, Moscow.

Algeo, T.J. and Heckel, P.H. 2008. The Late Pennsylvanian midcontinent sea of North America: A review. *Palaeogeography, Palaeoclimatology, Palaeoecology* 268: 205–221.

Barrick, J.E. and Boardman, D.R. 1989. Stratigraphic distribution of morphotypes of *Idiognathodus* and *Streptognathodus* in Missourian-lower Virgilian strata, north-central Texas. *In*: D.R. Boardman, J.E. Barrick, J.M. Cocke, and M.K. Nestell (eds.), Late Pennsylvanian Chronostratigraphic Boundaries in North-central Texas: Glacial-eustatic Events, Biostratigraphy, and Paleoecology. A Guidebook with Contributed Papers, part 2, Contributed Papers. *Texas Tech University Studies in Geology* 2: 167–188.

Barrick, J.E., Heckel, P.H., and Boardman, D.R. 2008. Revision of the conodont *Idiognathodus simulator* (Ellison, 1941), the marker species for the base of the Late Pennsylvanian global Gzhelian stage. *Micropaleontology* 54: 125–137.

Barrick, J.E., Lambert, L.L., Heckel, P.H., and Boardman, D.R. 2004. Pennsylvanian conodont zonation for Midcontinent North America. *Revista Española de Micropaleontologica* 36: 231–250.

Barrick, J.E., Lambert, L.L., Heckel, P.H., Rosscoe, S.J., and Boardman, D.R. 2013a. Midcontinent Pennsylvanian conodont zonation. *Stratigraphy* 10: 1–18.

Barrick, J.E., Lucas, S.G., and Kranier, K. 2013b. Conodonts of the Atrasado Formation (Uppermost Middle to Upper Pennsylvanian), Cerros de Amado region, central New Mexico, U.S.A. *In*: S.G. Lucas, W.J. Nelson, W.A. DiMichele, J.A. Spielmann, K. Krainer, J.E. Barrick, S. Elrick, and S. Voigt (eds.), Carboniferous–Permian Transition in cen-

tral New Mexico. *Museum of Natural History and Science Bulletin* 59: 239–252.

Barrick, J.E., Qi., Y., and Wang, Z. 2010. Latest Moscovian to earliest Gzhelian (Pennsylvanian) conodont faunas from the Naqing (Nashui) section, South Guizhou, China. *In*: X. Wang, Y. Qi, J. Groves, J.E. Barrick, T.I. Nemirovskaya, K. Ueno, and Y. Wang (eds.), *Carboniferous Carbonate Successions from the Shallow Marine to Slope in Southern Guizhou. Guidebook for the Field Excursions of the SCCS Workshops on GSSPs of the Carboniferous System*, 78–107. Nanjing Institute of Geology and Paleontology, Chinese Academy of Science, Nanjing.

Barksov, I.S. and Alekseev, A.S. 1975. Middle and Upper Carboniferous conodonts of the Moscow area [in Russian]. *Izvestiâ Akademii Nauk SSSR, Seriâ Geologičeskaâ* 6: 84–99.

Barskov, I.S., Alekseev, A.S., Kononova, L.I., and Migdisova, A.V. 1987. *Opredelitel konodontov verhnego Devona i Karbona*. 142 pp. Izdatel'stvo Moskovskogo Universiteta, Moskva.

Barskov, I.S., Isakova, T.N., and Schastlivtseva, P.N. 1981. Conodonts of boundary layers of gzhel'skii and assel'skii stages (southern Urals). *Proceedings of the USSR Academy of Sciences* 5: 78–87.

Bassler, R.S. 1925. Classification and stratigraphic use of the conodonts. *Geological Society of America Bulletin* 36: 128–220.

Boardman, D.R. 1999. Virgilian and lowermost Permian sea-level curve and cyclothems. *In*: P.H. Heckel (ed.), Guidebook, Fieldtrip 8, XIV International Congress on the Carboniferous–Permian. *Kansas Geological Survey, Open-file Report* 99 (27): 103–118.

Boardman, D.R. and Heckel, P.H. 1989. Glacial-eustatic sea-level curve for early Late Pennsylvanian sequence in north-central Texas and biostratigraphic correlation with curve for midcontinent North America. *Geology* 17: 802–805.

Boardman, D.R., Heckel, P.H., and Work, D.M. 2006. Conodont and ammonoid distribution of proposed Kasimovian–Gzhelian boundary in lower Virgilian strata in North American Midcontinent. *Newsletter on Carboniferous Stratigraphy* 4: 29–34.

Bookstein, F.P. 1991. *Morphometric Tools for Landmark Data: Geometry and Biology*. 435 pp. Cambridge University Press, Cambridge.

Branson, E.B. 1938. The conodont genus *Icriodus* and its stratigraphic distribution. *Journal of Paleontology* 12: 156–166.

Chernykh, V.V. [Černyh, V.V.] 1986. Conodonts from the Carboniferous–Permian boundary deposits of the western Urals [in Russian]. *In*: G.N. Papulov (ed.), *Pograničnye otloženiâ Karbona i Permi Urala, Priuralâ i srednej Azji*, 129–130. Institut geologii i geofizyki, Ural'skoye Otdeleniye Akademiya Nauk U.S.S.R., Moskva.

Chernykh, V.V. [Černyh, V.V.] 2005. *Zonalnoe metody v biostratigrafii. Zonalnaâ škala nižnej Permi po konodontam*. 217 pp. Institut geologii i geofizyki, Ural'skoye Otdeleniye Akademiya Nauk U.S.S.R., Ekaterinburg.

Chernykh, V.V. [Černyh, V.V.] 2012. *Atlas fauny i flory srednego-pozdnego Karbona Baškirii*. 156 pp. Institut geologii i geochemii, Ural'skoye Otdeleniye Akademiya Nauk U.S.S.R., Sverdlovsk.

Chernykh, V.V. [Černyh, V.V.] and Reshetkova, N.P. [Rešetkova, N.P.] 1987. *Biostratigrafiâ i konodonty pograničnyh otloženii Karbona i Permi zapadnogo sklona ûžnogo i Srednego Urala.* 45 pp. Institut geologii i geochemii, Ural'skoye Otdeleniye Akademiya Nauk U.S.S.R. Sverdlovsk.

Chernykh, V.V., Chuvashov, B.I., Davydov, V.I., Schmitz, M., and Snyder, W.S. 2006. Usolka section (southern Urals, Russia): a potential candidate for GSSP to define the base of the Gzhelian Stage in the global chronostratigraphic scale. *Geologija* 49: 204–217.

Corradini, C., Spalletta, C., Kaiser, S.I., and Matyja, H. 2013. Overview of conodonts across the Devonian/Carboniferous boundary. *In*: G.L. Albanesi and G. Ortega (eds.), Conodonts of the Andes. *Asociación Paleontológica Argentina, Publicación Especial* 13: 13–16.

Davydov, V.I., Chernykh, V.V, Chuvashov, B.I., Schmitz, M., and Snyder, W.S. 2008. Faunal assemblage and correlation of the Kasimovian–Gzhelian transition at Usolka section, southern Urals, Russia (a potential candidate for the GSSP to define base of Gzhelian Stage). *Stratigraphy* 5: 113–135.

Davydov, V.I., Crowley J.L., Schmitz, M.D., and Poletaev, V.I. 2010. High-precision U-Pb zircon age calibration of the global Carboniferous time scale and Milankovitch band cyclicity in the Donets Basin, eastern Ukraine. *Geochemistry, Geophysics, Geosystems* 2: 1–22.

Depecker, M., Berge, C., Penin, X., and Renous, S. 2006. Geometric morphometrics of the shoulder girdle in extant turtles (Chelonii). *Journal of Anatomy* 208: 35–45.

Donoghue, P.C.J. and Purnell, M.A. 1999. Mammal-like occlusion in conodonts. *Paleobiology* 25: 58–74.

Douglas, M.E., Douglas, M.R., Lynch, J.M., and McElroy, D.M. 2001. Use of geometric morphometrics to differentiate *Gila* (Cyprinidae) within the Upper Colorado River basin. *Copeia* 2001 (2): 389–400.

Dzik, J. 1976. Remarks on the evolution of Ordovician conodonts. *Acta Palaeontologica Polonica* 21: 395–455.

Ellison, S.P. 1941. Revision of the Pennsylvanian conodonts. *Journal of Paleontology* 15: 107–143.

Ellison, S.P. and Graves, R.W. 1941. Lower Pennsylvanian (Dimple limestone) conodonts of the Marathon region, Texas. *Missouri University School of Mines and Metallurgy* 14 (3): 1–21.

Goreva, N.V. and Alekseev, A.S. 2010. Upper Carboniferous conodont zones of Russia and their global correlation. *Stratigraphy and Geological Correlation* 18: 35–45.

Gunnell, F.H. 1931. Conodonts from the Fort Scott limestone of Missouri. *Journal of Paleontology* 5: 244–252.

Harris, R.W. and Hollingsworth, R.V. 1933. New Pennsylvanian conodonts from Oklahoma. *American Journal of Science, Series 5* 25: 193–204.

Heckel, P.H. 1986. Sea-level curve for Pennsylvanian eustatic marine transgressive-regressive depositional cycles along midcontinent outcrop belt, North America. *Geology* 14: 330–334.

Heckel, P.H. 1989. Updated Middle–Upper Pennsylvanian eustatic sea-level curve for Midcontinent North America and preliminary biostratigraphic characterization. *In*: Y. Jin and C. Li (eds.), XI International Carboniferous Congress 1987. *Compte Rendu, Academica Sinica, Beijing* 4: 160–185.

Heckel, P.H. 1994. Evaluation of evidence for glacio-eustatic control over marine Pennsylvanian cyclothems in North America and consideration of possible tectonic effects. *In*: J.M. Dennison and F.R. Ettensohn (eds.), Tectonic and Eustatic Controls on Sedimentary Cycles. *SEPM Concepts in Sedimentology and Paleontology* 4: 65–87.

Heckel, P.H. 1999. Overview of Pennsylvanian (Upper Carboniferous) stratigraphy in midcontinent region of North America. *In*: P.H. Heckel (eds.), Guidebook, Fieldtrip 8, XIV International Congress on the Carboniferous–Permian. *Kansas Geological Survey, Open-file Report* 99: 68–102.

Heckel, P.H. 2002. Genetic stratigraphy and conodont biostratigraphy of upper Desmoinesian–Missourian (Pennsylvanian) cyclothem succession in Midcontinent North America. *In*: L.V. Hills, C.M. Henderson, and E.W. Bamber (eds.), The Carboniferous and Permian of the World. *Canadian Society of Petroleum Geologists Memoir* 19: 99–119.

Heckel, P.H. 2008. Pennsylvanian cyclothems in Midcontinent North America as far-field effetcs of waxing and waning of Gondwana ice sheets. *In*: C.R. Fielding, T.D. Frank, and J.L. Isbell (eds.), Resolving the Late Paleozoic Ice Age in Time and Space. *Geological Society of America Special Paper* 442: 275–289.

Heckel, P.H. 2013. Pennsylvanian stratigraphy of Northern Midcontinent Shelf and biostratigraphic correlation of cyclothems. *Stratigraphy* 10: 3–39.

Heckel, P.H., Alekseev, A.S., Barrick, J.E., Boardman, D.R., Goreva, N.V., Isakova, T.N., Nemyrovska, T.I., Ueno, K., Villa, E., and Work, D.M. 2008. Choice of conodont *Idiognathodus simulator* (sensu stricto) as the event marker for the base of the global Gzhelian Stage (Upper Pennsylvanian Series, Carboniferous System). *Episodes* 31: 319–325.

Henderson, C.M., Pinard, S., and Beauchamp, B. 1995. Biostratigraphic and sequence stratigraphic relationships of Upper Carboniferous conodont and foraminfer distribution, Canadian Arctic Archipelago. *Bulletin of Canadian Petroleum Geology* 43: 226–246.

Jennings, T.V. 1959. Faunal zonation of the Minnelusa Formation, Black Hills, South Dakota. *Journal of Paleontology* 33: 986–1000.

Jones, D., Evans, A.R., Siu, K.K.W., Rayfield, E.J., and Donoghue, P.C.J. 2012. The sharpest tools in the box? Quantitative analysis of conodont element functional morphology. *Proceedings of the Royal Society* 279: 2849–2854.

Kaiser, S.I. and Corradini, C. 2011. The early siphonodellids (Conodonta, Late Devonian–Early Carboniferous): overview and taxonomic state. *Neues Jahrbuch für Geologie und Paläontologie Abhandlungen* 261: 19–35.

Klingenberg, C.P. 2011. MorphoJ: an integrated software package for geometric morphometrics. *Molecular Ecology Resources* 11: 353–357.

Kozitskaya, R.I. [Kozitskaâ, R.I.] 1983. Conodonts of the Upper Carboniferous deposits of the Dnieper–Donets Basin [in Russian]. *Izvestiâ Akademii Nauk SSSR Seriâ Geologičeskaâ* 11: 69–79.

Kozitskaya, R.I. and Nemirovskaya, T.I. 1997. Middle Carboniferous–Lower Permian conodonts from the Russian Platform. *In*: R.H. Wagner, C.F. Prins, and L.F. Granados (eds.), The Carboniferous of the World III, The Former USSR, Mongolia, Middle Eastern Platform, Afghanistan, and Iran. *Instituto Tecnológio GeoMinero de España Publication* 33: 295–296.

Kozitskaya, R.I. [Kozitskaâ, R.I.], Kossenko, Z.A., Lipnyagov, O.M. [Lipnâgov, O.M.], and Nemyrovskaya, T.A. [Nemyrovskaâ, T.A.] 1978. *Konodonty karbona Donetskogo bassejna*. 136 pp. Naukova Dumka, Akademiâ Nauk Ukrainskoj SSR, Kiev.

Lane, H.R. 1968. Symmetry in conodont element-pairs. *Journal of Paleontology* 42: 1258–1263.

Lane, H.R. and Straka, J.J. 1974. Late Mississippian and Early Pennsylvanian conodonts, Arkansas and Oklahoma. *Geological Society of America, Special Paper* 152: 1–144.

Martínez-Pérez, C., Plasencia, P., Jones, D., Kolar-Jurkovšek, T., Sha, J., Botella, H., and Donoghue, P.C.J. 2014a. There is no general model for occlusal kinematics in conodonts. *Lethaia* 47: 547–555.

Martínez-Pérez, C., Rayfield, E.J., Purnell, M.A., and Donoghue, P.C.J. 2014b. Finite element, occlusal, microwear and microstructural analyses indicate that conodont microstructure is adapted to dental function. *Paleontology* 57: 1059–1066.

Purnell, M.A. and Jones, D. 2012. Quantitative analysis of conodont tooth wear and damage as a test of ecological and functional hypotheses. *Paleobiology* 38: 605–626.

Purnell, M.A., Donoghue, P.C.J., and Aldridge, R.J. 2000. Orientation and anatomical notation in conodonts. *Journal of Paleontology* 74: 113–122.

Ritter, S.M. 1995. Upper Missourian–Lower Wolfcampian (upper Kasimovian–Lower Asselian) conodont biostratigraphy of the Midcontinent, U.S.A. *Journal of Paleontology* 69: 1139–1154.

Rholf, F.J. 1990. Morphometrics. *Annual Reviews of Ecology and Systematic* 21: 299–316.

Rohlf, F.J. 2010a. *TpsDig, Version 2.16*. Department of Ecology and Evolution, State University of New York, Stony Brook. http://life.bio.sunysb.edu/morph/

Rohlf, F.J. 2010b. *TpsUtil, Version 1.46*. Department of Ecology and Evolution, State University of New York, Stony Brook. http://life.bio.sunysb.edu/morph/

Rholf, F.J. and Marcus, L.F. 1993. A revolution in morphometrics. *Trends in Ecology and Evolution* 8: 129–132.

Rholf, F.J. and Slice, D. 1990. Extension of the Procrustes method for the optimal superimposition of landmarks. *Systematic Zoology* 39: 40–59.

Rosscoe, S.J. 2008. Idiognathodus *and* Streptognathodus *species from the Lost Branch to Dewey sequences (Middle–Upper Pennsylvanian) of the Midcontinent Basin, North America*. 200 pp. Unpublished Ph.D. Dissertation, Texas Tech University, Lubbock.

Rosscoe, S.J. and Barrick, J.E. 2009. Revision of *Idiognathodus* species from the Desmoinesian–Missourian (Moscovian–Kasimovian) boundary interval in the Midcontinent Basin, North America. *In*: D.J. Over (ed.), Conodont Studies Commemorating the 150th Anniversary of the First Conodont Paper (Pander, 1856) and the 40th Anniversary of the Pander Society. *Paleontographica Americana* 62: 115–147.

Rosscoe, S.J. and Barrick, J.E. 2013. North American species of the conodont genus *Idiognathodus* from the Moscovian–Kasimovian boundary composite sequence and correlation of the Moscovian–Kasimovian stage boundary. *In*: S.G. Lucas, W.A. DiMichelle, J.E. Barrick, J.W. Schneider, and J.A. Spielmann (eds.), The Carboniferous–Permian Transition. *New Mexico Museum of Natural History and Science, Bulletin* 60: 1–18.

Sanz-López, J. and Blanco-Ferrera, S. 2013. Early Evolution of *Declinognathodus* close to the Mid-Carboniferous boundary interval in the Barcaliente type section (Spain). *Palaeontology* 56: 927–946.

Sanz-López, J., García-López, S., and Sánchez de Posada, L.C. 2006. The Mid-Carboniferous boundary in Northern Spain: difficulties for correlation of the Global Stratotype Section and Point. *Rivista Italiana di Paleontologia e Stratigrafia* 112: 3–22.

Sobolev, N.N. and Nakrem, H.A. 1996. Middle Carboniferous–Lower Permian conodonts of Novaya Zemlya. *Norsk Polarinstitutt Skrifter* 199: 1–129.

Stauffer, C.R. and Plummer, H.J. 1932. Texas Pennsylvanian conodonts and their stratigraphic relations. *University of Texas, Bulletin* 3201: 13–50.

Strauss, R.E. 2010. Discriminating groups of organisms. *In*: E. Ashraf (eds.), Morphometrics for Nonmorphometricians. *Lecture Notes in Earth Sciences* 124: 73–91.

Sudar, M., Jovanović, D., Stojanović, S., Filipović, I., and Gajić, R. 2007. Late Pennsylvanian conodont biostratigraphy of the Krive Reka Formation from the Jadar Block, Vardar Zone (NW Serbia). *Journal of Alpine Geology* 48: 101–115.

Von Bitter, P.H. 1972. *Environmental Control of Conodont Distributions in the Shawnee Group (Upper Pennsylvanian) of Eastern Kansas*. 105 pp. The University of Kansas Paleontological Institute, Lawrence.

Wang, Z. and Qi, Y. 2003. Upper Carboniferous conodonts from South Guizhou of China. *Rivista Italiana di Paleontologia e Stratigrafia* 109: 379–397.

Zagorodnyuk, P.A. [Zagorodnûk, P.A.], Alksenem A.E., Degtyarev, D.D. [Degtârev, D.D.], Alekasandrov, V.A., Kochetkova, N.M. [Kočetkova, N.M.], Yagudina, Z.G. [Âgudina, Z.G.], Yelysheva, R.S. [Elyševa, R.S.], Polyarnaya, Z.A. [Polârnaâ, Z.A.], Konstantinenko, L.I., and Furduy, R.S. 1979. *Atlas fauny i flory srednego-pozdnego Karbona Baškirii*. 110–199. Izdatel'stvo Nedra, Moskva.

Zelditch, M.L., Swiderski, D.L., Sheets, H.D., and Fink, W.L. 2004. *Geometric Morphometrics for Biologists: A Primer*. 437 pp. Elsevier Academic Press, New York.

Appendix 1

Locality information.

Old Sedan spillway: 37°10'5.78" N, 96°13'1.91" W, outcrop is located in the creek behind a building for a small day camp.

Clinton Dam: 38°56'33.25" N, 95°19'46.93" W, outcrop is located on the north end of a walking park, underneath Clinton Parkway.

I-229 roadcut: 39°51'18.10" N, 94°51'37.94" W, exposure is on the west side of highway I-229, about 0.1 miles north of the overpass with route 375.